Title

Adventitial Fibroblasts Induce a Distinct Proinflammatory/Profibrotic Macrophage Phenotype in Pulmonary Hypertension

Journal

The Journal of Immunology, 193(2)

ISSN

0022-1767

Authors

El Kasmi, Karim C
Pugliese, Steven C
Riddle, Suzette R
et al.

Publication Date

2014-07-15

DOI

10.4049/jimmunol.1303048

Peer reviewed

Published in final edited form as:
J Immunol. 2014 July 15; 193(2): 597–609. doi:10.4049/jimmunol.1303048.

Adventitial Fibroblasts induce a distinct Pro-inflammatory/Pro-fibrotic Macrophage Phenotype in Pulmonary Hypertension

Karim C. El Kasmi[1,*], **Steven C. Pugliese**[2], **Suzette R. Riddle**[2], **Jens M. Poth**[2], **Aimee L. Anderson**[1], **Maria G. Frid**[2], **Min Li**[2], **Soni S. Pullamsetti**[3], **Rajkumar Savai**[3], **Maria A. Nagel**[4], **Mehdi A. Fini**[2], **Brian B. Graham**[5], **Rubin M. Tuder**[5], **Jacob E. Friedman**[6], **Holger K. Eltzschig**[7], **Ronald J. Sokol**[1], and **Kurt R. Stenmark**[2,*]

[1]Department of Pediatrics, Division of Gastroenterology, Hepatology and Nutrition, University of Colorado Denver, School of Medicine, Aurora, CO 80045

[2]Department of Pediatrics and Medicine, Division of Critical Care Medicine/Cardiovascular Pulmonary Research Laboratories, University of Colorado Denver, School of Medicine, Aurora, CO 80045

[3]Max-Planck Institute for Heart and Lung Research, Department of Lung Development and Remodeling and University of Giessen and Marburg Lung Center (UGMLC), member of the German Center for Lung Research (DZL), Bad Nauheim, Germany

[4]Department of Neurology, University of Colorado Denver, School of Medicine, Aurora, CO 80045

[5]Department of Medicine, University of Colorado Denver, School of Medicine, Aurora, CO 80045

[6]Department of Pediatrics, Division of Biochemistry and Molecular Genetics, University of Colorado Denver, School of Medicine, Aurora, CO 80045

[7]Department of Anesthesiology, University of Colorado Denver, School of Medicine, Aurora, CO 80045

Abstract

Macrophage accumulation is not only a characteristic hallmark but also a critical component of pulmonary artery (PA) remodeling associated with pulmonary hypertension (PH). However, the cellular and molecular mechanisms that drive vascular macrophage activation and their functional phenotype remain poorly defined. Utilizing multiple levels of in vivo (bovine and rat models of hypoxia-induced PH, together with human tissue samples) and in vitro (primary mouse, rat, and bovine macrophages, human monocytes, as well as primary human and bovine fibroblasts) approaches, we observed that adventitial fibroblasts derived from hypertensive Pas (bovine and human) regulate macrophage activation. These fibroblasts activate macrophages through paracrine IL6 and STAT3, HIF1, and C/EBPβ signaling to drive expression of genes previously implicated in chronic inflammation, tissue remodeling, and PH. This distinct fibroblast-activated macrophage

[*]To whom correspondence should be addressed: Karim C. El Kasmi; Karim.Elkasmi@UCDenver.edu; Phone: (303) 859-6318; Fax: (303) 724-5628, Kurt R. Stenmark; Kurt.Stenmark@UCDenver.edu; Phone: (303) 724-5620; Fax: (303) 724-5628.

Author contributions: Conception, hypotheses delineation, design of the study, analysis and interpretation of data, preparation of manuscript (KCE, KRS); data acquisition, experimentation, provision of reagents and technical assistance (SRR, HKE, ALA, MGF, ML, SSP, SP, RS, MAN, BAM, AF, MF, JMP, BGB); substantial involvement in manuscript preparation (JEF, RJS).

phenotype was independent of IL4/IL13-STAT6 and TLR-MyD88 signaling. We found that genetic STAT3 haplodeficiency in macrophages attenuated macrophage activation while complete STAT3 deficiency increased macrophage activation through compensatory upregulation of STAT1 signaling, while deficiency in C/EBPβ or HIF1 attenuated fibroblast driven macrophage activation. These findings challenge the current paradigm of IL4/IL13-STAT6 mediated alternative macrophage activation as the sole driver of vascular remodeling in PH and uncover a crosstalk between adventitial fibroblasts and macrophages in which paracrine IL6 activated STAT3, HIF1, and C/EBPβ signaling is critical for macrophage activation and polarization. Thus, targeting IL6 signaling in macrophages by completely inhibiting C/EBPβ, HIF1a or partially inhibiting STAT3 may hold therapeutic value for treatment of PH and other inflammatory conditions characterized by increased IL6 and absent IL4/IL13 signaling.

Introduction

Studies in animal models of PH and humans with PAH have provided convincing evidence that early and persistent inflammation is an essential component of pulmonary vascular disease (1–7). The extent of the vascular inflammatory infiltrate in PH has been shown to directly correlate with parameters of vascular remodeling and hemodynamics (3, 4, 6). Importantly, as described extensively by our group and others, PH-associated vascular inflammation is largely perivascular/adventitial in nature, and is characterized by a robust influx of leukocytes, primarily macrophages, into the adventitial compartment (3, 5, 8–12). An essential role for these cells in the PH process was demonstrated in experiments where *in vivo* depletion of macrophages attenuated pulmonary vascular remodeling (8). We have documented that in both experimental hypoxia-induced PH and human PAH, the PA adventitia harbors activated fibroblasts (termed here PH-Fibs) with a hyper-proliferative, apoptosis-resistant, and pro-inflammatory phenotype (the latter defined by increased generation of IL6, IL1β, CCL2/MCP1, CCL12/SDF1, VCAM1, osteopontin) that are involved in macrophage recruitment, retention, and activation (10, 12–17). We have further demonstrated that the pro-inflammatory phenotype of PH-Fibs remains persistent *ex vivo* over numerous passages in cell culture and is regulated through epigenetic mechanisms involving alterations in histone deacetylase activity and miRNA expression (16, 17). In line with this paradigm, we found that PH-Fibs recruit, retain, and activate naïve macrophages (17). However, neither the exact phenotype induced nor the signaling pathways involved in the polarization of macrophages in sterile forms of PH have been identified.

Tissue remodeling and fibrotic-angiogenic responses in chronic inflammatory conditions, including PH, have long been associated with “alternative activation” of macrophages (12, 18–20). The current paradigm holds that IL4/IL13 signaling and STAT6-regulated alternative activation of macrophages (AAM) are important in the vascular remodeling process in some forms of PH and in other fibrosing/tissue remodeling conditions where Th2 responses are prominent (21–26). Recent reports have, however, documented that STAT3 signaling can also play a key role in chronic inflammatory diseases in which tissue remodeling is prominent (27–34). Further, recent studies strongly support a spectrum model of macrophage activation where macrophage phenotype is dependent on specific signals

present in the inflammatory microenvironment, rather than simply classic “M1” vs “M2” (35).

IL6 has been identified as a major activator of STAT3 signaling in macrophages and IL6-STAT3 signaling promotes an activation profile distinct from that in IL4/IL13-induced alternative activation of macrophages (36–38). IL6 signaling has recently been shown to drive fibrosis and unresolved inflammation in the peritoneum in the absence of IL4, IL13, and TGFβ (39). Further, many reports have documented increased serum and lung concentrations of IL6 in patients with PH (31, 40, 41). A pathogenic role for IL6 in the pathogenesis of certain forms of PH is supported by observations that IL6 knockout mice are protected from PH (32) while IL6 transgenic mice develop spontaneous PH and vascular remodeling (30).

We thus sought to examine the hypothesis that certain forms of PH, including those associated with chronic hypoxia, are characterized by the presence of a fibroblast-activated macrophage that exhibits a unique phenotype dependent on IL6 and STAT3 signaling and distinct from the canonical alternatively (IL4/IL13) activated macrophage phenotype. Our approach was to examine the phenotype of macrophages both *in vivo* using models of severe hypoxia-induced PH and patients with PAH and in vitro by examining the effects of fibroblasts derived from animals and humans with PH on macrophage phenotype signaling. Herein, we show that fibroblast-derived paracrine IL6 and macrophage STAT3 in conjunction with HIF1 and C/EBPβ signaling, and not IL4/IL13-STAT6, are pivotal in mediating activation of macrophages by adventitial fibroblasts from the pulmonary hypertensive vessel. Further, these fibroblast activated macrophages express genes previously implicated in the pathogenesis of PH and associated with chronic non-resolving and fibrosing tissue responses. Thus, fibroblast-mediated macrophage activation and STAT3, HIF1, and C/EBPβ signaling downstream of IL6 may be important elements underlying certain forms of PH.

Materials and Methods

Immunohistological/immunoflourescence staining and laser-capture microdissection (LCM)

Frozen OCT-embedded sections of human lung specimens from control subjects (n = 4) and patients with idiopathic pulmonary arterial hypertension (iPAH, n = 5) were provided by Dr. Barbara Meyrick (Vanderbilt University, Transplant Procurement Center) via the Pulmonary Hypertension Breakthrough Initiative funded by the Cardiovascular Medical Research Education Fund. Additional human tissue, paraffin embedded, (n=5 donor controls and n=5 iPAH) was provided by S.S. Pullamsetti, a member of the German Center for Lung Research (DLZ). Patient descriptions for this tissue was provided previously in our recent manuscript (16). Immunostaining was performed according to standard protocols.

Human lung tissue specimens from subjects with iPAH (n = 8) or donors (n = 7) were obtained during lung transplantation. Tissue specimens were from patients previously utilized and described in another study by us (16). Intrapulmonary arteries (50–100 μm diameter) were micro-dissected under optical control using the Laser micro-dissection

device LMD6000 (Leica, Wetzlar, Germany) and collected in Eppendorf tubes containing RNA lysis buffer. Total mRNA was extracted from human micro-dissected vessels using RNeasy Micro Kit (QIAGEN, Hilden, Germany). Reverse transcription PCR was performed using the iScript cDNA Synthesis Kit (BioRad, Munich, Germany). Real-time PCR was performed using iQ SYBR Green Supermix according to the manufacturer's instructions (BioRad, Munich, Germany) and with a Mx3000P (Stratagene, Heidelberg, Germany). Intron-spanning primers were designed using sequence information from the NCBI database. Ct values were normalized to the endogenous control (porphobilinogen deaminase, *PBGD*).

The study protocol for tissue donation was approved by the Ethics Committee (Ethik Kommission am Fachbereich Humanmedizin der Justus Liebig Universität Giessen) of the University Hospital Giessen (Giessen, Germany) in accordance with National Law and with Good Clinical Practice/International Conference on Harmonisation guidelines. Written informed consent was obtained from each patient or their next-of-kin (AZ 31/93).

Animals

1-day-old calves were exposed to hypobaric hypoxia (P_B=445 mmHg) for 2 weeks (n=7); age-matched controls (n=7) were kept at ambient altitude (P_B=640 mmHg). Wistar-Kyoto rats (8 weeks old) were exposed to hypobaric hypoxia (P_B = 380 mmHg) for 4 weeks (n = 9); age-matched controls (n = 9) were kept at ambient altitude. Standard veterinary care was according to institutional guidelines in compliance with IACUC-approved protocols.

Bone marrow-derived macrophages

Mouse bone marrow-derived macrophages (BMDMs) were generated from *Il4*$^{-/-}$/*Il13*$^{-/-}$, *IL4ra*$^{-/-}$, *Stat6*$^{-/-}$, *Myd88*$^{-/-}$, *C/ebpβ*$^{-/-}$, *Stat3*$^{fl/fl}$;Tie2cre, *Stat3*$^{fl/+}$;Tie2cre, and *Stat3*$^{+/+}$;Tie2cre mice (a gift from P. Murray; St. Jude Children's Research Hospital, Memphis, TN), *Hif1α*$^{fl/fl}$;LysMcre were bred in house. C57BL/6 and Balb/c mice (purchased from Jackson Laboratory, Bar Harbor, ME). All mice were on a C57BL/6 background except for *Il4ra*$^{-/-}$ mice (Balb/c). Rat BMDM were generated from Sprague-Dawley rats. Bovine BMDMs were isolated from healthy calves and grown in complete Iscove's DMEM with 20% FBS and human M-CSF (50 ng/ml). When bovine BMDM cultures were initiated from frozen bone marrow cells, live cells were obtained using negative column selection (Dead Cell Removal Kit, Miltenyi, Auburn, CA) and incubated for 24 h with human (due to limited availability of bovine-specific) cytokines, Stem cell factor (50 ng/ml), IL3 (20 ng/ml), and IL6 (50 ng/ml) before exposure to MCSF. All BMDM were cultured in recombinant murine or bovine MCSF (100ng/ml) for 7 days prior to use.

Adventitial fibroblasts

Adventitial fibroblasts from distal pulmonary arteries of calves (control or with PH) were isolated by explant culture as described (16, 17). Consistent with our previous observations (17), fibroblasts from chronically hypoxic hypertensive calves (PH-Fibs) were significantly smaller in size than those from controls (CO-Fibs) and proliferated at markedly higher rates as previously shown (16). The PH-Fibs utilized for study exhibited modest alpha-smooth

muscle actin immunoreactivity, and were HSP-47 and vimentin positive. These cells at the time of study lacked expression of smooth muscle myosin heavy chain and lacked expression of CD34, CD14, and CD68. Human adventitial fibroblasts were a kind gift from Nick Morrell (University of Cambridge, UK). HFL-1 human fetal lung fibroblasts were purchased from ATCC. Experiments were performed on cells at passages 4–10. Conditioned medium was collected from confluent fibroblast cultures and used to treat BMDMs or the THP-1 monocyte cell line (ATCC, Manassas, VA).

For Transwell (Corning, Tewksbury, MA) experiments, distal pulmonary vessels (1–3 mm outer diameter) were isolated from either control or pulmonary hypertensive calf lungs and left whole or separated into medial and adventitial layers prior to dissecting into 3-mm^2 pieces for incubation in the upper chamber, above naïve mouse BMDM for 16 hrs. Adjacent tissue pieces were used for whole and separated tissue. Three tissue pieces from each animal were used per experiment.

All cytokines were purchased from BD Biosciences (San Jose, CA), Cell Signaling (Danvers, MA), Milltenyi Biotech (Auburn, CA), eBiosciences (San Diego, CA), or Kingfisher Biotech (St Paul, MN). Ultrapure LPS was purchased from Sigma.

Immunoblotting

Cells were lysed in M-PER (Thermo-Fisher) containing protease and phosphatase inhibitors (Thermo-Fisher). Protein lysates were separated by 4–15% gradient SDS-PAGE in Tris-HCl buffer and transferred to nitrocellulose membranes. Membranes were blocked in 3% milk in Tris-buffered saline containing 0.05% Tween. Antibodies included: mouse monoclonal anti-Arg1 antibody (1:2000, BD Biosciences, San Jose, CA); rabbit polyclonal anti-total STAT1, pSTAT1, total STAT3, pSTAT3, total STAT6, pSTAT6 (1:1000, Cell Signaling Technology); and mouse monoclonal anti-GAPDH (1:1000, Santa Cruz).

IL6 protein detection

Human IL6 was quantified in cell culture supernatant using a human IL6 multiplex sandwich ELISA with electrochemiluminescence detection on the Meso Scale Discovery Platform (Meso Scale Discovery, Rockville, MD) as per the manufacturer's protocol on a SECTOR Imager 2400A (http://www.mesoscale.com). Quantitative detection range in our analysis for IL-6 was 0.6– 9,871.4 pg/ml. Bovine IL6 was quantified using an ELISA development kit from Kingfisher Biotech, St. Paul, MN) according to manufacturer's instructions and standard ELISA procedures. Recombinant bovine IL6 was used as a standard.

Quantitative reverse transcriptase-polymerase chain reaction (qRT-PCR)

RNA was isolated using Trizol reagent (Invitrogen, Grand Island, NY) or the Qiagen RNeasy kit (Valencia, CA) according to the manufacturer's instructions. First-strand cDNA synthesis was performed using iScript cDNA Synthesis Kit (BioRad, Hercules, CA). qRT-PCRs were performed using TaqMan probes and reagents from Applied Biosystems according to the manufacturer's instructions. Gene expression was calculated after normalization to Hprt1 using the Δ/Δ Ct method.

Statistical analysis

GraphPad Prism software was used to determine significance. Student's t-test was used to compare two groups. One-way ANOVA and Bonferroni's correction for multiple comparisons were used to compare more than two groups.

Results

Expression of the STAT3 regulated proteins CD163 and CD206 on macrophages is observed *in vivo* in humans and animals with PH

We first sought to define the adventitial macrophage phenotype *in situ* in humans, and in several animal models of PH. Macrophage CD163 and CD206 expression has been reported in various chronic inflammatory/fibrotic tissue responses (42, 43). CD163 is a STAT3-regulated gene (44) and CD206 can be activated through either IL6-STAT3 or IL4-STAT6 (Supplementary Fig. 1A). We thus chose to examine *in situ* expression of CD163 and CD206 on adventitial macrophages. Consistent with previous reports we detected pronounced adventitial accumulation of macrophages (defined as cells positive for the pan-macrophage marker CD68) in the PA of patients with idiopathic pulmonary artery hypertension (iPAH), calves with hypoxia-induced PH, and rats with hypoxia or monocrotaline (MCT)-induced PH (Supplementary Fig. 1B and C) (3–6) Furthermore, the PA of humans, calves, and rats with PH revealed markedly increased numbers of CD163+ cells, which were specifically localized to the adventitia (Fig. 1A and Supplementary Fig. 1C). In order to attribute CD163 and also CD206 staining to macrophages, the PA adventitia from calves with hypoxia-induced PH was stained with the typical macrophage marker MHCII. ~90% of MHCII+ cells co-expressed the macrophage-specific marker CD68 as detected by double-staining and confocal microscopy. In addition, the majority (75%) of CD163+ and CD206+ cells also co-expressed MHCII (Supplementary Fig. 1D). CD163 positive cells in the PA adventitia from calves with hypoxia-induced PH also expressed the canonical STAT3-regulated protein SOCS3 (Supplementary Fig. 1E). Moreover, we detected increased adventitial protein expression of phosphorylated STAT3 in PAs from patients with iPAH (Fig. 1B), which was paralleled by detection of increased mRNA (laser capture dissection) of the canonical STAT3-regulated genes *SOCS3* and *IL4Ra* (Fig. 1C) together with increased protein and mRNA expression of the STAT3 activating cytokine IL6 (Fig. 1B & C). Notably, we did not detect mRNA for the STAT6 activating cytokines *IL4* or *IL13* in PAs from calves, humans, and rats with PH **(not shown)**.

These results demonstrate that in various species and multiple models of PH, macrophages consistently accumulate within the PA adventitia, the site of active vascular remodeling, and stereotypically express surface markers associated with a pro-remodeling phenotype and consistent with activation through IL6-STAT3 signaling.

Adventitial fibroblasts mediate macrophage activation

We next sought to determine the cell type(s) and mechanism(s) responsible for adventitial macrophage activation towards this phenotype, hypothesizing that the PA adventitia was the vascular compartment most capable of activating these macrophages. Exposure of naïve primary bone marrow derived macrophages (BMDMs) *in vitro* to intact whole PA explants

from calves with hypoxia-induced PH significantly increased transcription of *Cd163, Cd206, Il4ra, and Socs3* (Fig. 2A). Removal of adventitia from the PA explant resulted in marked decreased mRNA expression in BMDMs. However, the adventitia alone induced an identical response to that observed with whole PA explants (Fig. 2A). These findings were confirmed in a separate experiment using bovine BMDMs (data not shown). These results demonstrate that during vascular remodeling in PH, cells within the remodeled PA adventitia produce soluble factors that can activate primary naïve macrophages toward a gene expression phenotype that is identical to the one observed on adventitial macrophages *in situ*.

To test whether pro-inflammatory PA adventitial fibroblasts (16, 17) were the cellular source of soluble factors inducing this macrophage phenotype, we exposed naïve BMDMs to conditioned media (CM) generated by *ex vivo*-cultured human (from patients with iPAH) or bovine (from hypoxic calves with PH) adventitial fibroblasts. Remarkably, CM from both bovine and human PH-Fibs significantly increased transcription of *Cd163*, *Cd206*, *Socs3*, and *Il4rα* in naïve macrophages (mouse and bovine) and THP-monocytes in comparison to the transcript amounts induced by CM from CO-Fibs (adventitial fibroblasts isolated from human or bovine controls). Additionally, CM from bovine PH-Fibs also induced similar gene expression in mouse and rat (data not shown) naïve macrophages indicating that this signaling mechanism is effective across species (Fig. 2B and Supplementary Fig. 2). Thus, within the remodeled PA adventitia of animals and humans with PH, activated fibroblasts provide the soluble factors that induce this macrophage phenotype.

Fibroblast activated adventitial macrophages do not exhibit a canonical alternatively activated phenotype

Macrophage expression of CD163 and CD206 in fibrosis and tissue remodeling is thought to reflect a canonical alternatively activated macrophage (AAM) phenotype (42, 45, 46) as defined by IL4/IL13-IL4Ra-STAT6-dependent signaling (47). We therefore sought to determine if the functional programming of adventitial macrophages by the PA adventitia and PA adventitial fibroblasts involved IL4/IL13-IL4Rα-STAT6 signaling. Accordingly, we examined transcription of canonical STAT6-regulated genes whose combined expression in macrophages has traditionally been viewed to reflect the AAM phenotype (*Arg1* encoding Arginase1, *Chi3l3* encoding Chitinase-3-like protein 3/YM1, and *Retnla* encoding Resistin-like molecule Relmα/FIZZ1) (19, 47). We discovered that soluble factors released by intact whole PA explants or by isolated PA adventitia (both containing fibroblasts) derived from calves with chronic hypoxia-induced PH significantly increased transcription of *Arg1* but not of *Chi3l3* and *Retnla* in mouse macrophages. PA explants from which the adventitia was removed (absence of fibroblasts) failed to induce significant expression of any gene (Fig. 3A). In addition, CM produced by cells isolated from the adventitia of animals (bovine) or humans with PH (PH-Fib) replicated this gene expression pattern in mouse, rat, and bovine BMDMs (Fig. 3B & C, Supplementary Fig. 3A). The absence of *Chi3l3* and *Retnla* mRNA induction in mouse macrophages was not due to an inability to respond to IL4 and was also not limited to a particular time point (Supplementary Fig. 3B).

Furthermore, compared to control fibroblasts, neither human nor bovine PH-Fibs had increased transcription for *IL4* or *IL13*, and neither human nor bovine PH-Fib CM contained detectable amounts of IL4 or IL13 protein **(not shown)**. In addition, neither bovine nor human PH Fib CM induced transcription of another canonical STAT6-regulated AAM gene, *TGM2/Tgm2* **(not shown)**. Moreover, we discovered that PH-Fib CM induced Arginase1 protein expression in mouse, rat, and bovine macrophages in the absence of STAT6 phosphorylation but instead in the presence of STAT3 phosphorylation (Supplementary Fig. 3C, D, E). Additionally, *Arg1* mRNA expression in PH-Fib CM-activated macrophages did not require paracrine or autocrine IL4/IL13 signaling because expression of *Arg1* was similar in macrophages from IL4/IL13 double-deficient mice (unresponsive to autocrine IL4/IL13), IL4R α−/− mice (unresponsive to paracrine and autocrine IL4 and IL13), and STAT6-deficient mice (unable to upregulate *Arg1* in response to IL4/IL13) in response to bovine PH-Fib CM (Fig. 3D). Because *Arg1* can also be induced in response to TLR-MyD88 signaling (48) and C/EBPβ signaling (36, 48, 49), we exposed naïve mouse macrophages from WT, *Myd88*$^{-/-}$, and *C/ebpβ*$^{-/-}$ mice to bovine PH-Fib CM. While *Arg1* expression was similar in WT and *MyD88*$^{-/-}$ macrophages (Fig. 3E), *C/ebpβ*$^{-/-}$ macrophages showed dramatically reduced *Arg1* expression (Fig. 3F). These results demonstrate that PH-Fib-activated macrophages were not alternatively activated through the IL4/IL13-STAT6 pathway and that neither the IL4/IL13/IL4R/STAT6 nor the MyD88 (microbe- and danger-associated signals and IL1) pathway underlies *Arg1* expression; instead, STAT3 and C/EBPβ play a critical role.

PH-Fibs activate macrophages through paracrine IL6

As IL6 activates STAT3 signaling in macrophages, which in turn can activate C/EBPβ (36, 37), we next examined whether paracrine, fibroblast-derived IL6 could be responsible for the macrophage activation. Increased IL6 and phosphorylated STAT3 protein expression in the PAs from patients (Fig1B), along with evidence of STAT3 signaling in adventitial macrophages (Supplemental Figures 1E (SOCS3 staining), & 4), supported the idea that IL6 was the most likely paracrine cytokine to activate STAT3 signaling in fibroblast activated macrophages. We found that adventitial fibroblasts from from calves with PH generated IL6 protein **and** *IL6* mRNA (Fig.4A). siRNA knockdown of *IL6* expression in bovine PH-Fibs led to reduction in IL6 protein in the CM (Fig. 4B) which resulted in significant attenuation of the CM-induced transcriptional upregulation of STAT3 regulated genes in naïve mouse macrophages (Fig. 4C). In addition, expression of these genes was not reduced in IL6-deficient macrophages in response to PH-Fib CM (Fig. 4D) ruling out any potential contribution of autocrine IL6 signaling to the activation of STAT3 signaling in fibroblast-activated macrophages.

PIM1 and NFATC2 signaling is promoted in fibroblast-activated macrophages

We next tested if this IL6-STAT3-regulated fibroblast-activated macrophage phenotype would also include expression of additional functional STAT3-regulated genes that have previously been associated with the pathogenesis of PH, such as *Pim1*, and *Nfatc2* (33, 34). Gene expression analysis using laser-capture micro-dissection of PAs from patients with iPAH revealed up-regulation of mRNA for *PIM1* and *NFATC2* (Fig. 5A). In addition, intact whole PA and PA adventitia from PH calves induced transcription of *Pim1* and *Nfatc2* in

naive mouse macrophages (Fig. 5B). Moreover, bovine PH-Fib CM induced *Pim1* and *Nfatc2* expression in naïve bovine (Fig. 5C), mouse (Fig. 5D), and rat macrophages (Fig. 5E). Human PH-Fib CM was also capable of inducing transcription of *PIM1* but not *NFATC2* in human monocytes **(not shown)**. PH-Fib CM induced expression of *Pim1* and *Nfatc2* was dependent on paracrine IL6 but not autocrine IL6 (Fig 5F & G). Finally, transcriptional induction of *Pim1*, *Nfatc2*, *Socs3* and *Il4ra* mRNA in mouse macrophages activated by bovine PH-Fib CM was independent of STAT6 or MyD88 (experiments performed in $Stat6^{-/-}$ and $MyD88^{-/-}$ BMDMs) **(not shown)**.

PH-Fib-activated macrophages demonstrate upregulated *Hif1a* and *Vegfa* mRNA

HIF1 can be induced through STAT3 (50). Gene expression analysis of PAs from patients with iPAH revealed up-regulation of *HIF1A* mRNA (Fig. 6A). Mouse macrophages exposed to whole intact PA and PA adventitia from calves with hypoxia-induced PH showed increased *Hif1a* mRNA expression (Fig. 6B). Bovine PH-Fib CM also induced transcription of *Hif1a* in naive mouse, rat, and bovine macrophages (Fig. 6C–E). Human PH-Fib CM also induced *HIF1A* mRNA in naive human monocytes (Fig. 6F). Notably, in mouse macrophages, this response was independent of autocrine IL6, STAT6 and MyD88 (experiments performed in $Il6^{-/-}$, $Stat6^{-/-}$ and $MyD88^{-/-}$ BMDMs), as well as hypoxia (experiments conducted under normoxic conditions) **(not shown)**.

HIF1 regulates expression of VEGFA, which has been implicated in the pathogenesis of PH. Mouse macrophages exposed to whole intact PA and PA adventitia from calves with hypoxia-induced PH showed increased *Vegfa* mRNA expression (Fig. 7A). Bovine PH-Fib CM also induced transcription of *Vegfa* in naive mouse, rat, and bovine macrophages (Fig. 7B–D). Human PH-Fib CM also induced *VEGFA* mRNA in naive human monocytes (Fig. 7E).

STAT3, HIF1, and C/EBPβ are critical regulators of PH-Fib mediated macrophage activation

The above results suggested that STAT3, C/EBPβ and HIF1 are central regulators of the fibroblast-activated and IL6-activated macrophage phenotype. We therefore examined their role in fibroblast and IL6 mediated macrophage activation by using a genetic approach. We first examined the role of STAT3 and used BMDMs from mice with conditional alleles of *Stat3* ($Stat3^{fl/fl}$ *(complete knockout)* and $Stat3^{fl/+}$ (haplo-deficiency, incomplete knockout)) crossed onto the Tie2cre background [mice lacking *Stat3* globally are embryo-lethal (51)]. As expected, BMDMs with haplodeficiency in STAT3 (from $Stat3^{fl/+;}$ *Tie2Cre* mice) displayed attenuated activation reflected by ~50% reduction in gene expression of STAT3 target genes in response to PH-Fib CM and recombinant bovine IL6 (Fig. 8A) and mouse recombinant IL6 (not shown). Unexpectedly, expression of STAT3 target genes was not attenuated in BMDMs with complete absence of STAT3, but instead increased in response to bovine PH-Fib CM (Fig. 8A). As reported previously, in murine fibroblasts with complete genetic absence of STAT3, IL6 stimulates STAT1 signaling. (52). We thus determined STAT1 and STAT3 signaling in WT BMDMs, in response to either IL6 or PH-Fib CM, and found that STAT1 was weakly phosphorylated and as expected STAT3 was strongly phosphorylated, demonstrating that the IL6 receptor can initiate both STAT3 and STAT1 signaling (Supplementary Fig. 4A). Consistent with this finding and the previously reported

data in mouse STAT3−/− fibroblasts, we found that in BMDMS with complete genetic absence of STAT3, IL6- and PH-Fib CM-induced increased and prolonged STAT1 phosphorylation in the absence of STAT3 phosphorylation (Supplementary Fig. 4A). Moreover, PH-Fib CM induced significantly higher transcript levels of the canonical STAT1-regulated genes *Ip10* and *Irf1* in BMDMs with complete STAT3-deficiency as compared to WT macrophages (Fig. 8B). In addition, in BMDMs with complete STAT3-deficiency, expression of *Ip10* and *Irf1* mRNA was increased in response to both IL6 and IFNγ (Fig. 8C), demonstrating that in the absence of STAT3, up-regulation of STAT1 signaling was not restricted to activation by the IL6 receptor. Moreover, we found that the anti-inflammatory properties of IL10 to suppress LPS mediated induction of IL1β was conserved in BMDMs with STAT3 haplo-deficiency while the anti-inflammatory properties of IL10 to suppress LPS mediated induction of IL1β were abrogated in BMDMs with complete STAT3 deficiency (Fig. 8D). These results indicated that STAT3 plays a critical role in the fibroblast-activated macrophage and that incomplete inhibition attenuates macrophage activation by IL6 and PH-Fib CM and conserves responsiveness to anti-inflammatory IL10, but that complete deletion of STAT3 promotes macrophage activation in response to IL6 through increased STAT1 signaling and in addition abrogates responsiveness to anti-inflammatory IL10

Based on the attenuated *Arg1* expression found in PH-Fib CM-activated C/EBPβ-deficient macrophages (Fig. 3F), we next examined the role of C/EBPβ in this STAT3-activated macrophage phenotype. *C/ebpβ* mRNA was robustly expressed in mouse, rat, and bovine macrophages after exposure to bovine and human PH-Fib CM (Supplementary Fig. 4B). Importantly, PH-Fib mediated expression of STAT3-regulated genes was significantly attenuated in macrophages with genetic deletion of *C/ebpβ* (Fig. 8E).

Finally, we determined the role of HIF1 signaling in IL6 mediated STAT3-regulated gene expression. For this purpose we used wild type (derived from $Hif1a^{+/+}$*; LysMcre)* and $Hif1a^{-/-}$ (derived from $Hif1a^{fl/fl}$*; LysMcre mice*) BMDMs and measured gene expression of the canonical STAT3-regulated gene *Arg1* in response to IL6. We found that IL6-induced expression of *Arg1* was significantly increased in the presence of HIF1 stabilization with DMOG demonstrating that HIF1 can directly promote STAT3 regulated gene expression. Genetic absence of HIF1 significantly reduced IL6-induced *Arg1* expression in both presence and absence of HIF stabilization (Fig. 8F), demonstrating a critical role for HIF1 in regulating IL6 mediated *Arg1* expression.

Discussion

Our studies provide evidence that: (1) in multiple animal models and humans with PH, macrophages accumulate specifically within the PA adventitia (a site of active vascular remodeling (12); (2) these adventitial macrophages stereotypically express CD163 and CD206; (3) the adventitial compartment is responsible for macrophage activation to this phenotype; (4) and adventitial fibroblasts are the responsible adventital cell that mediates macrophage activation toward a previously unrecognized and distinct alternative activation phenotype; (5) the mechanism of macrophage activation involves paracrine fibroblast derived IL6 and macrophage STAT3, C/EBPβ, and HIF1a signaling in the absence of IL4/

IL13-STAT6 as well as TLR/MyD88; (6) Targeting of C/EBPb and HIF1, and attenuation of but not annihilation of STAT3, reduces macrophage activation. Based on these findings we propose that in pulmonary vascular remodeling associated with PH adventitial fibroblast-mediated activation of macrophages via paracrine IL6 towards expression of a STAT3 signaling dependent pro-remodeling phenotype (42, 43, 45, 46) is a stereotypic and conserved response pattern in various species and forms of PH. Furthermore, cooperative signaling between STAT3, HIF1 and C/EBPβ in response to IL6 shapes a distinct macrophage phenotype.

Considering the reported pivotal role of macrophages in PA vascular remodeling in PH (8, 24, 53), our study suggests that adventitial macrophages expressing CD163/CD206 through STAT3 signaling are critical regulators of the vascular remodeling process in PH. Our study is the first to show that in vascular remodeling associated with PH, adventitial macrophages express CD163 and CD206 and that this phenotype can be induced by soluble factors generated by adventitial fibroblasts. Being that our study is the first to associate this macrophage phenotype with vascular remodeling and considering that studies examining the role of this macrophage phenotype functionally in fibrosing diseases are rare, we can only speculate with regard to its specific role in vascular remodeling. Christmann et al showed peripheral blood mononuclear cells from patients with scleroderma PH express higher levels of CD206 than in patients with scleroderma without PH and in healthy controls and correlated that CD206 expression with mean PA pressures and mortality (23). Nakayama et al found that in patients with scleroderma and elevated serum soluble CD163 (sCD163) levels, 70% of patients had an elevated RVSP on echo versus 28% of patients with normal levels (54). In patients with sickle cell disease and PH, soluble sCD163 levels were over twice that of sickle cell patients without PH (55).

Consistent with the restricted localization of macrophages with this phenotype to the adventitia, we found that the adventitia in the PA is the principal vascular compartment in which macrophages are activated towards this phenotype. Further, our findings demonstrate that conditioned media from cultured adventitial fibroblasts fully replicates the ability of the PA adventitia to activate macrophages and thus our study demonstrates that adventitial fibroblasts are likely the principal mediators of adventitial macrophage activation and phenotypic polarization. This finding also excludes the possibility that the activating ability of the adventitial fibroblast was an *in vitro* acquired artifact, and furthermore argues against a role for direct cell-to-cell contacts, including co-stimulatory molecules and antigen presentation. Finally, these observations justified using PH-Fib CM and naïve BMDMs for further *in vitro* analysis of the signaling pathways that were involved in activating macrophages.

Our study unexpectedly revealed no detectable *Il4* and *Il13* mRNA or IL4/IL13 protein in PA tissue from iPAH patients, calves or rats with PH, or in human and bovine PH-Fibs and PH-Fib CM. Consistent with the absence of IL4/IL13, no STAT6 signaling was detected in macrophages in response to PA adventitia or PH-Fib-CM, and the canonical STAT6-regulated genes *Chi3l3*, *Retnla*, and *Tgm2* were not expressed. The independence of this macrophage phenotype from STAT6 signaling demonstrates that these fibroblast-activated macrophages are not alternatively activated in the classical sense (19, 47). However, we

found that PA vessels, PA adventitia, and PH-Fib CM induced expression of *Arg1* (which is a canonical STAT6-regulated gene) in the absence of STAT6 phosphorylation in mouse, rat and bovine macrophages. Because Arginase1 (encoded by *Arg1*) is a macrophage product with important roles in tissue remodeling, including PH, and is thought to be a functional hallmark of AAM (48, 56) we examined the mechanism of its expression in fibroblast-activated macrophages in greater detail. *Arg1* can be induced in macrophages through multiple pathways: IL4/IL13-STAT6 signaling in which C/EBPβ plays a critical role (49), but also STAT6-independent signaling in which intracellular microbes engage TLR-MyD88-C/EBPβ pathways (48). This latter pathway involves generation of IL6 in infected macrophages, which in a paracrine fashion, induces *Arg1* through STAT3 signaling in uninfected bystander macrophages (36). Our data identify an additional pathway of *Arg1* expression in macrophages, which occurs in the absence of microbial infection or TLR-MyD88 signaling, is completely independent of IL4/IL13-STAT6 signaling, and instead is controlled by fibroblast-derived paracrine IL6 and macrophage STAT3, HIF1, and C/EBPβ. Arginase1 has been shown to promote fibrosis, including that in PH-associated vascular remodeling, by providing downstream metabolites that promote cell division, collagen synthesis and wound healing (25, 56). Higher Arginase1 levels are found in lungs of hypoxic mice (57), and Arginase1-expressing alveolar macrophages have been implicated in the pathogenesis of hypoxia-induced PH in mice (24). In contrast, macrophage Arginase1 plays neither a protective nor pathogenic role in TH2-mediated lung pathologies (58) but is important in suppression of fibrosis in TH2-mediated hepatic and intestinal pathologies (56, 59, 60). Our study proves that Arginase1 in macrophages can be expressed in the absence of microbes and TH2 responses. Thus, macrophage Arginase1 may promote or inhibit fibrosis in a disease/trigger context and organ/compartment-specific manner. Consequently, fibroblast-mediated persistent expression of Arginase1 in vascular macrophages may promote vascular remodeling in PH and possibly in tissue remodeling in various pathologies in the absence of microbial triggers and TH2-mediated inflammation.

In addition to IL4/IL13, which can be involved in the classic TH2-mediated pulmonary vascular remodeling seen in asthma or schistosomiasis (18, 26), IL6 plays a major role in vascular remodeling associated with certain forms of PH as indicated by our detection of high IL6 levels in PAs from patients with PH together with phosphorylated STAT3 and expression of canonical STAT3-regulated genes. Note that adventitial macrophages in the PA of hypoxic calves co-expressed SOCS3 and the STAT3-regulated protein CD163, and that PH-Fibs expressed high levels of IL6. Moreover, explanted PA adventitial tissue, as well as bovine and human PH-Fib CM, induced an identical STAT3-regulated gene expression pattern in naïve human, bovine, mouse and rat macrophages. Importantly, the STAT3-regulated gene expression pattern was attenuated in macrophages in response to CM from siRNA-IL6 treated PH-Fibs. These findings are consistent with the pivotal role of IL6 in various mouse models of pulmonary remodeling/fibrosis, including models in which mice overexpressing IL6 display severe hypoxia-induced PH accompanied by inflammatory vascular remodeling, while mice genetically deficient in IL6 are protected from PH (30, 32).

Recent studies have reported that *src*-induced STAT3-PIM1-NFACTc2 signaling enhances proliferation and resistance to apoptosis in smooth muscle cells during PH-associated

vascular remodeling, although the role of IL6 was not addressed (33, 34). Here, we found that consistent with the known role of IL6 in activating STAT3 in macrophages (37), STAT3 signals in PH can be regulated through IL6 and that PIM1 and NFACTc2 expression in macrophages can be mediated by fibroblast-derived IL6. The incomplete attenuation of *Pim1* and *Nfatc2* expression in macrophages in response to CM from siRNA-IL6-treated PH-Fibs raises the possibility that intracellular signaling pathways through *src* contribute to IL6-induced STAT3 signaling in macrophages and that enhanced proliferation and apoptosis resistance in the vessel wall, are also controlled by fibroblast-derived IL6 in any IL6-responsive cell, including fibroblasts, macrophages, endothelial cells and smooth muscle cells. We and others have proposed that intercellular signaling pathways originating in the PA adventitia may be essential in promoting medial and intimal changes in the vascular remodeling process (12). The observation that expression of IL6, STAT3, and IL4Ra was not limited to the PA adventitia supports IL6-STAT3 signaling as a mechanism of cross-talk between the different compartments of the vascular wall.

PH-Fib CM-activated macrophages also expressed *Hif1α* and *Vegfα*, factors critically involved in PH tissue remodeling and vascularization (61, 62). This finding led us to hypothesize that HIF1 plays a critical role in IL6-STAT3 mediated gene expression. We thus tested the isolated effect of IL6 on expression of Arginase1 in the presence or absence of HIF1. We made the novel observation that HIF1 plays a critical role in regulating expression of Arg1 in response to IL6. Thus, HIF1 may fine-tune IL6-STAT3 signaling regulated gene expression in macrophages but also other cells within the vessel wall that are responsive to IL6. Because HIF1 is downstream of STAT3, IL6 induced STAT3 might thus serve as a central hub for the coordination of gene expression patterns that are involved in inflammation (HIF1, Arg1, Socs3), remodeling (Arg1), metabolism (HIF1), proliferation and apoptosis (Pim1, Nfatc2), and vascularization (Vegfa). This hypothesis is furthermore supported by the recent observation that transcription of Vegf can be cooperatively regulated by STAT3 and HIF1 (63, 64). Moreover, analysis of the STAT3 promoter revealed HIF binding sites (unpublished data), thus a feed forward signaling loop between HIF and STAT3 might drive persistent activation of STAT3 regulated genes in response to IL6.

We therefore hypothesized that genetic deficiency of STAT3 would attenuate the IL6 and PH-Fib activated macrophage phenotype, which would be consistent with the proposed role of STAT3 inhibition as a therapeutic approach in treating PH (33, 34, 65). We observed that activation of BMDMs with genetic haplo-deficiency in Stat3 in response to PH-Fib CM and recombinant IL6 was attenuated, consistent with a critical role for STAT3 in promoting this macrophage phenotype. However, we also made the important observation that complete genetic blockade of STAT3 signaling in IL6 and PH-Fib stimulated macrophages resulted in increased activation (increase in expression of STAT3-regulated genes) which was associated with increased and prolonged STAT1 phosphorylation and increased expression of canonical STAT1-regulated pro-inflammatory genes. These findings prompted the question of how STAT3 regulated genes can be up-regulated in the absence of STAT3 protein. A previous study had demonstrated that genetic deletion of STAT3 in IL6 stimulated mouse fibroblasts also resulted in increased and prolonged phospho-STAT1 signaling and up-regulation of STAT1 target genes STAT3 target genes (i.e. Arginase1)

(52). These findings together with our results demonstrate that in the complete absence of STAT3, IL6 signaling enhances expression of both STAT1 and STAT3 regulated genes in fibroblasts and macrophages through increased and prolonged STAT1 signaling. Similarly, a previous study has demonstrated that in the genetic absence of STAT1, macrophages express increased amounts of STAT3 regulated genes (66). These studies together with our findings highlight that STAT1 and STAT3 can "cross-regulate" gene expression. In addition, our data also demonstrate that anti-inflammatory IL10 signaling is abrogated in the complete absence of STAT3 but fully preserved in incomplete inhibition of STAT3 findings that are consistent with the reported non-redundant role of STAT3 in mediating the IL10-regulated anti-inflammatory response in macrophages and the principal role of macrophages in mediating IL10-STAT3 anti-inflammatory signaling (67). Thus our data are consistent with reported STAT3 inhibition studies that show attenuation of PH in animal models but also suggest that complete STAT3 blockade may render any IL6-responsive cell within the vessel wall, including fibroblasts, refractory to anti-inflammatory IL10 and promote persistent pro-inflammatory STAT1 mediated activation in response to paracrine IL6 (33, 34). It thus remains to be determined if STAT3 blockade is a safe approach for treatment of PH.

We next focused on signaling pathways downstream of STAT3 that were involved in promoting this macrophage phenotype and thus could be additional candidate therapeutic targets. We found that genetic absence of C/EBPβ or HIF1a (both transcription factors associated with pro-inflammatory activation of macrophages and both STAT3 target genes) attenuated macrophage activation in response to IL6 and PH-Fib CM which was paralleled by attenuated transcription of STAT3 target genes. This finding is consistent with the reported synergistic function of C/EBPβ and HIF1 with STATs (49, 63, 64, 68) and with studies indicating a role for C/EBPβ in regulating macrophage activation in obesity, wound healing, and ischemic heart injury (36, 48,49, 69–71). Importantly, unlike the consequences of completely blocking STAT3, the IL10-meditated anti-inflammatory response is fully functional in the absence of C/EBPβ and HIF1 **(unpublished observations and personal communication with Peter Murray)**. Thus, targeting C/EBPβ and/or HIF1 may effectively mitigate IL6-mediated remodeling in various pathologies, such as PH and rheumatoid arthritis. Analysis of the therapeutic potential of STAT3 vs. C/EBPβ or HIF1 inhibition on vascular remodeling awaits the examination of animal models with cell type-specific ablation of STAT3, HIF1 and C/EBPβ.

Collectively, our data identify an intercellular signaling mechanism in the PA adventitia that is controlled by fibroblast-mediated signaling in various species and forms of PH and that shapes macrophage differentiation towards a distinct phenotype critically regulated through IL6, STAT3, HIF1, and C/EBPβ in the absence of pathogens, danger signals, and TH2 cytokines. Based on the independence of this macrophage phenotype from TLR-MyD88 and STAT6 signaling, and considering the critical role of STAT3 signaling, together with the role of fibroblast-generated paracrine signals, chiefly IL6, in controlling this phenotype, we conclude that these STAT3-activated macrophages portray a distinct functional phenotype representing its own category of macrophage activation that is crucial in pathological tissue remodeling. This intercellular signaling axis among IL6, fibroblasts and STAT3-activated

macrophages might be important in other chronic fibrotic inflammatory conditions that occur in the absence of TH2- derived cytokines and pathogens, such as scleroderma, rheumatoid arthritis, acute respiratory distress syndrome and fibrotic lung disease.

Supplementary Material

Refer to Web version on PubMed Central for supplementary material.

Acknowledgments

We thank Peter Murray, PhD, at St. Jude Children's Research Hospital for providing the STAT3-deficient bone marrow and for critically reviewing the manuscript. We thank Michael Yeager, PhD, and Kelly Colvin for help with immunostaining PAs from hypoxic and MCT-treated rats. Confocal imaging was performed at Advance Light Microscopy Core, University of Colorado Denver.

This work was supported in part by NIH Axis Grant 1R01 HL114887-02, Program Project Grant 5P01 HL014985-39, and Training Grant 2T32 HL07171-36.

JMP was supported by grant D/10/52531 from the German Academic Exchange Service (DAAD).

References

1. Morrell NW, Archer SL, Defelice A, Evans S, Fiszman M, Martin T, Saulnier M, Rabinovitch M, Schermuly R, Stewart D, Truebel H, Walker G, Stenmark KR. Anticipated classes of new medications and molecular targets for pulmonary arterial hypertension. Pulmonary circulation. 2013; 3:226–244. [PubMed: 23662201]
2. Price LC, Wort SJ, Perros F, Dorfmuller P, Huertas A, Montani D, Cohen-Kaminsky S, Humbert M. Inflammation in pulmonary arterial hypertension. Chest. 2012; 141:210–221. [PubMed: 22215829]
3. Savai R, Pullamsetti SS, Kolbe J, Bieniek E, Voswinckel R, Fink L, Scheed A, Ritter C, Dahal BK, Vater A, Klussmann S, Ghofrani HA, Weissmann N, Klepetko W, Banat GA, Seeger W, Grimminger F, Schermuly RT. Immune and inflammatory cell involvement in the pathology of idiopathic pulmonary arterial hypertension. American journal of respiratory and critical care medicine. 2012; 186:897–908. [PubMed: 22955318]
4. Stacher E, Graham BB, Hunt JM, Gandjeva A, Groshong SD, McLaughlin VV, Jessup M, Grizzle WE, Aldred MA, Cool CD, Tuder RM. Modern age pathology of pulmonary arterial hypertension. American journal of respiratory and critical care medicine. 2012; 186:261–272. [PubMed: 22679007]
5. Stenmark KR, Meyrick B, Galie N, Mooi WJ, McMurtry IF. Animal models of pulmonary arterial hypertension: the hope for etiological discovery and pharmacological cure. American journal of physiology. Lung cellular and molecular physiology. 2009; 297:L1013–L1032. [PubMed: 19748998]
6. Tuder RM, Voelkel NF. Pulmonary hypertension and inflammation. The Journal of laboratory and clinical medicine. 1998; 132:16–24. [PubMed: 9665367]
7. Tuder RM, Archer SL, Dorfmuller P, Erzurum SC, Guignabert C, Michelakis E, Rabinovitch M, Schermuly R, Stenmark KR, Morrell NW. Relevant issues in the pathology and pathobiology of pulmonary hypertension. Journal of the American College of Cardiology. 2013; 62:D4–D12. [PubMed: 24355640]
8. Frid MG, Brunetti JA, Burke DL, Carpenter TC, Davie NJ, Reeves JT, Roedersheimer MT, van Rooijen N, Stenmark KR. Hypoxia-induced pulmonary vascular remodeling requires recruitment of circulating mesenchymal precursors of a monocyte/macrophage lineage. The American journal of pathology. 2006; 168:659–669. [PubMed: 16436679]
9. Hassoun PM, Mouthon L, Barbera JA, Eddahibi S, Flores SC, Grimminger F, Jones PL, Maitland ML, Michelakis ED, Morrell NW, Newman JH, Rabinovitch M, Schermuly R, Stenmark KR, Voelkel NF, Yuan JX, Humbert M. Inflammation, growth factors, and pulmonary vascular

remodeling. Journal of the American College of Cardiology. 2009; 54:S10–S19. [PubMed: 19555853]

10. Stenmark KR, Frid MG, Yeager M, Li M, Riddle S, McKinsey T, El Kasmi KC. Targeting the adventitial microenvironment in pulmonary hypertension: A potential approach to therapy that considers epigenetic change. Pulmonary circulation. 2012; 2:3–14. [PubMed: 22558514]
11. Stenmark KR, Nozik-Grayck E, Gerasimovskaya E, Anwar A, Li M, Riddle S, Frid M. The adventitia: Essential role in pulmonary vascular remodeling. Comprehensive Physiology. 2011; 1:141–161. [PubMed: 23737168]
12. Stenmark KR, Yeager ME, El Kasmi KC, Nozik-Grayck E, Gerasimovskaya EV, Li M, Riddle SR, Frid MG. The adventitia: essential regulator of vascular wall structure and function. Annual review of physiology. 2013; 75:23–47.
13. Anwar A, Li M, Frid MG, Kumar B, Gerasimovskaya EV, Riddle SR, McKeon BA, Thukaram R, Meyrick BO, Fini MA, Stenmark KR. Osteopontin is an endogenous modulator of the constitutively activated phenotype of pulmonary adventitial fibroblasts in hypoxic pulmonary hypertension. American journal of physiology. Lung cellular and molecular physiology. 2012; 303:L1–L11. [PubMed: 22582113]
14. Das M, Burns N, Wilson SJ, Zawada WM, Stenmark KR. Hypoxia exposure induces the emergence of fibroblasts lacking replication repressor signals of PKCzeta in the pulmonary artery adventitia. Cardiovascular research. 2008; 78:440–448. [PubMed: 18218684]
15. Panzhinskiy E, Zawada WM, Stenmark KR, Das M. Hypoxia induces unique proliferative response in adventitial fibroblasts by activating PDGFbeta receptor-JNK1 signalling. Cardiovascular research. 2012; 95:356–365. [PubMed: 22735370]
16. Wang D, Zhang H, Li M, Frid MG, Flockton AR, McKeon BA, Yeager ME, Fini MA, Morrell NW, Pullamsetti SS, Velegala S, Seeger W, McKinsey TA, Sucharov CC, Stenmark KR. MicroRNA-124 controls the proliferative, migratory, and inflammatory phenotype of pulmonary vascular fibroblasts. Circulation research. 2014; 114:67–78. [PubMed: 24122720]
17. Li M, Riddle SR, Frid MG, El Kasmi KC, McKinsey TA, Sokol RJ, Strassheim D, Meyrick B, Yeager ME, Flockton AR, McKeon BA, Lemon DD, Horn TR, Anwar A, Barajas C, Stenmark KR. Emergence of fibroblasts with a proinflammatory epigenetically altered phenotype in severe hypoxic pulmonary hypertension. Journal of immunology. 2011; 187:2711–2722.
18. Duffield JS, Lupher M, Thannickal VJ, Wynn TA. Host responses in tissue repair and fibrosis. Annu Rev Pathol. 2013; 8:241–276. [PubMed: 23092186]
19. Murray PJ, Wynn TA. Protective and pathogenic functions of macrophage subsets. Nat Rev Immunol. 2011; 11:723–737. [PubMed: 21997792]
20. Wynn TA, Barron L. Macrophages: master regulators of inflammation and fibrosis. Seminars in liver disease. 2010; 30:245–257. [PubMed: 20665377]
21. Angelini DJ, Su Q, Yamaji-Kegan K, Fan C, Teng X, Hassoun PM, Yang SC, Champion HC, Tuder RM, Johns RA. Resistin-like molecule-beta in scleroderma-associated pulmonary hypertension. American journal of respiratory cell and molecular biology. 2009; 41:553–561. [PubMed: 19251945]
22. Yamaji-Kegan K, Su Q, Angelini DJ, Myers AC, Cheadle C, Johns RA. Hypoxia-induced mitogenic factor (HIMF/FIZZ1/RELMalpha) increases lung inflammation and activates pulmonary microvascular endothelial cells via an IL-4-dependent mechanism. J Immunol. 2010; 185:5539–5548. [PubMed: 20889544]
23. Christmann RB, Hayes E, Pendergrass S, Padilla C, Farina G, Affandi AJ, Whitfield ML, Farber HW, Lafyatis R. Interferon and alternative activation of monocyte/macrophages in systemic sclerosis-associated pulmonary arterial hypertension. Arthritis and rheumatism. 2011; 63:1718–1728. [PubMed: 21425123]
24. Vergadi E, Chang MS, Lee C, Liang OD, Liu X, Fernandez-Gonzalez A, Mitsialis SA, Kourembanas S. Early macrophage recruitment and alternative activation are critical for the later development of hypoxia-induced pulmonary hypertension. Circulation. 2011; 123:1986–1995. [PubMed: 21518986]
25. Wynn TA. Fibrotic disease and the T(H)1/T(H)2 paradigm. Nature reviews. Immunology. 2004; 4:583–594. [PubMed: 15286725]

26. Graham BB, Chabon J, Kumar R, Kolosionek E, Gebreab L, Debella E, Edwards M, Diener K, Shade T, Bifeng G, Bandeira A, Butrous G, Jones K, Geraci M, Tuder RM. Protective role of IL-6 in vascular remodeling in schistosoma pulmonary hypertension. American journal of respiratory cell and molecular biology. 2013; 49:951–959. [PubMed: 23815102]
27. Knight DA, Ernst M, Anderson GP, Moodley YP, Mutsaers SE. The role of gp130/IL-6 cytokines in the development of pulmonary fibrosis: critical determinants of disease susceptibility and progression? Pharmacology & therapeutics. 2003; 99:327–338. [PubMed: 12951164]
28. Natsume M, Tsuji H, Harada A, Akiyama M, Yano T, Ishikura H, Nakanishi I, Matsushima K, Kaneko S, Mukaida N. Attenuated liver fibrosis and depressed serum albumin levels in carbon tetrachloride-treated IL-6-deficient mice. Journal of leukocyte biology. 1999; 66:601–608. [PubMed: 10534116]
29. Ash Z, Emery P. The role of tocilizumab in the management of rheumatoid arthritis. Expert opinion on biological therapy. 2012; 12:1277–1289. [PubMed: 22849354]
30. Steiner MK, Syrkina OL, Kolliputi N, Mark EJ, Hales CA, Waxman AB. Interleukin-6 overexpression induces pulmonary hypertension. Circulation research. 2009; 104:236–244. 228p following 244. [PubMed: 19074475]
31. Soon E, Holmes AM, Treacy CM, Doughty NJ, Southgate L, Machado RD, Trembath RC, Jennings S, Barker L, Nicklin P, Walker C, Budd DC, Pepke-Zaba J, Morrell NW. Elevated levels of inflammatory cytokines predict survival in idiopathic and familial pulmonary arterial hypertension. Circulation. 2010; 122:920–927. [PubMed: 20713898]
32. Savale L, Tu L, Rideau D, Izziki M, Maitre B, Adnot S, Eddahibi S. Impact of interleukin-6 on hypoxia-induced pulmonary hypertension and lung inflammation in mice. Respir Res. 2009; 10:6. [PubMed: 19173740]
33. Paulin R, Courboulin A, Meloche J, Mainguy V, Dumas de la Roque E, Saksouk N, Cote J, Provencher S, Sussman MA, Bonnet S. Signal transducers and activators of transcription-3/pim1 axis plays a critical role in the pathogenesis of human pulmonary arterial hypertension. Circulation. 2011; 123:1205–1215. [PubMed: 21382889]
34. Paulin R, Meloche J, Jacob MH, Bisserier M, Courboulin A, Bonnet S. Dehydroepiandrosterone inhibits the Src/STAT3 constitutive activation in pulmonary arterial hypertension. American journal of physiology. Heart and circulatory physiology. 2011; 301:H1798–H1809. [PubMed: 21890685]
35. Xue J, Schmidt SV, Sander J, Draffehn A, Krebs W, Quester I, De Nardo D, Gohel TD, Emde M, Schmidleithner L, Ganesan H, Nino-Castro A, Mallmann MR, Labzin L, Theis H, Kraut M, Beyer M, Latz E, Freeman TC, Ulas T, Schultze JL. Transcriptome-based network analysis reveals a spectrum model of human macrophage activation. Immunity. 2014; 40:274–288. [PubMed: 24530056]
36. Qualls JE, Neale G, Smith AM, Koo MS, DeFreitas AA, Zhang H, Kaplan G, Watowich SS, Murray PJ. Arginine usage in mycobacteria-infected macrophages depends on autocrine-paracrine cytokine signaling. Science signaling. 2010; 3:ra62. [PubMed: 20716764]
37. El Kasmi KC, Holst J, Coffre M, Mielke L, de Pauw A, Lhocine N, Smith AM, Rutschman R, Kaushal D, Shen Y, Suda T, Donnelly RP, Myers MG Jr, Alexander W, Vignali DA, Watowich SS, Ernst M, Hilton DJ, Murray PJ. General nature of the STAT3-activated anti-inflammatory response. Journal of immunology. 2006; 177:7880–7888.
38. Lang R, Pauleau AL, Parganas E, Takahashi Y, Mages J, Ihle JN, Rutschman R, Murray PJ. SOCS3 regulates the plasticity of gp130 signaling. Nat Immunol. 2003; 4:546–550. [PubMed: 12754506]
39. Fielding CA, Jones GW, McLoughlin RM, McLeod L, Hammond VJ, Uceda J, Williams AS, Lambie M, Foster TL, Liao CT, Rice CM, Greenhill CJ, Colmont CS, Hams E, Coles B, Kift-Morgan A, Newton Z, Craig KJ, Williams JD, Williams GT, Davies SJ, Humphreys IR, O'Donnell VB, Taylor PR, Jenkins BJ, Topley N, Jones SA. Interleukin-6 signaling drives fibrosis in unresolved inflammation. Immunity. 2014; 40:40–50. [PubMed: 24412616]
40. Humbert M, Monti G, Brenot F, Sitbon O, Portier A, Grangeot-Keros L, Duroux P, Galanaud P, Simonneau G, Emilie D. Increased interleukin-1 and interleukin-6 serum concentrations in severe primary pulmonary hypertension. American journal of respiratory and critical care medicine. 1995; 151:1628–1631. [PubMed: 7735624]

41. Yoshio T, Masuyama JI, Kohda N, Hirata D, Sato H, Iwamoto M, Mimori A, Takeda A, Minota S, Kano S. Association of interleukin 6 release from endothelial cells and pulmonary hypertension in SLE. The Journal of rheumatology. 1997; 24:489–495. [PubMed: 9058654]

42. Ikezumi Y, Suzuki T, Karasawa T, Hasegawa H, Yamada T, Imai N, Narita I, Kawachi H, Polkinghorne KR, Nikolic-Paterson DJ, Uchiyama M. Identification of alternatively activated macrophages in new-onset paediatric and adult immunoglobulin A nephropathy: potential role in mesangial matrix expansion. Histopathology. 2011; 58:198–210. [PubMed: 21323947]

43. Mathai SK, Gulati M, Peng X, Russell TR, Shaw AC, Rubinowitz AN, Murray LA, Siner JM, Antin-Ozerkis DE, Montgomery RR, Reilkoff RA, Bucala RJ, Herzog EL. Circulating monocytes from systemic sclerosis patients with interstitial lung disease show an enhanced profibrotic phenotype. Lab Invest. 2010; 90:812–823. [PubMed: 20404807]

44. Weaver LK, Pioli PA, Wardwell K, Vogel SN, Guyre PM. Up-regulation of human monocyte CD163 upon activation of cell-surface Toll-like receptors. Journal of leukocyte biology. 2007; 81:663–671. [PubMed: 17164428]

45. Higashi-Kuwata N, Makino T, Inoue Y, Takeya M, Ihn H. Alternatively activated macrophages (M2 macrophages) in the skin of patient with localized scleroderma. Exp Dermatol. 2009; 18:727–729. [PubMed: 19320738]

46. Bacci M, Capobianco A, Monno A, Cottone L, Di Puppo F, Camisa B, Mariani M, Brignole C, Ponzoni M, Ferrari S, Panina-Bordignon P, Manfredi AA, Rovere-Querini P. Macrophages are alternatively activated in patients with endometriosis and required for growth and vascularization of lesions in a mouse model of disease. The American journal of pathology. 2009; 175:547–556. [PubMed: 19574425]

47. Gordon S. Alternative activation of macrophages. Nat Rev Immunol. 2003; 3:23–35. [PubMed: 12511873]

48. El Kasmi KC, Qualls JE, Pesce JT, Smith AM, Thompson RW, Henao-Tamayo M, Basaraba RJ, Konig T, Schleicher U, Koo MS, Kaplan G, Fitzgerald KA, Tuomanen EI, Orme IM, Kanneganti TD, Bogdan C, Wynn TA, Murray PJ. Toll-like receptor-induced arginase 1 in macrophages thwarts effective immunity against intracellular pathogens. Nature immunology. 2008; 9:1399–1406. [PubMed: 18978793]

49. Gray MJ, Poljakovic M, Kepka-Lenhart D, Morris SM Jr. Induction of arginase I transcription by IL-4 requires a composite DNA response element for STAT6 and C/EBPbeta. Gene. 2005; 353:98–106. [PubMed: 15922518]

50. Dang EV, Barbi J, Yang HY, Jinasena D, Yu H, Zheng Y, Bordman Z, Fu J, Kim Y, Yen HR, Luo W, Zeller K, Shimoda L, Topalian SL, Semenza GL, Dang CV, Pardoll DM, Pan F. Control of T(H)17/T(reg) balance by hypoxia-inducible factor 1. Cell. 2011; 146:772–784. [PubMed: 21871655]

51. Takeda K, Noguchi K, Shi W, Tanaka T, Matsumoto M, Yoshida N, Kishimoto T, Akira S. Targeted disruption of the mouse Stat3 gene leads to early embryonic lethality. Proc Natl Acad Sci U S A. 1997; 94:3801–3804. [PubMed: 9108058]

52. Costa-Pereira AP, Tininini S, Strobl B, Alonzi T, Schlaak JF, Is'harc H, Gesualdo I, Newman SJ, Kerr IM, Poli V. Mutational switch of an IL-6 response to an interferon-gamma-like response. Proc Natl Acad Sci U S A. 2002; 99:8043–8047. [PubMed: 12060750]

53. Tuder RM, Stacher E, Robinson J, Kumar R, Graham BB. Pathology of pulmonary hypertension. Clinics in chest medicine. 2013; 34:639–650. [PubMed: 24267295]

54. Nakayama W, Jinnin M, Makino K, Kajihara I, Makino T, Fukushima S, Inoue Y, Ihn H. Serum levels of soluble CD163 in patients with systemic sclerosis. Rheumatol Int. 2012; 32:403–407. [PubMed: 21120485]

55. Tantawy AA, Adly AA, Ismail EA. Soluble CD163 in young sickle cell disease patients and their trait siblings: a biomarker for pulmonary hypertension and vaso-occlusive complications. Blood Coagul Fibrinolysis. 2012; 23:640–648. [PubMed: 22885767]

56. Campbell L, Saville CR, Murray PJ, Cruickshank SM, Hardman MJ. Local Arginase 1 activity is required for cutaneous wound healing. J Invest Dermatol. 2013

57. Jin Y, Calvert TJ, Chen B, Chicoine LG, Joshi M, Bauer JA, Liu Y, Nelin LD. Mice deficient in Mkp-1 develop more severe pulmonary hypertension and greater lung protein levels of arginase in

response to chronic hypoxia. Am J Physiol Heart Circ Physiol. 2010; 298:H1518–H1528. [PubMed: 20173047]

58. Barron L, Smith AM, El Kasmi KC, Qualls JE, Huang X, Cheever A, Borthwick LA, Wilson MS, Murray PJ, Wynn TA. Role of arginase 1 from myeloid cells in th2-dominated lung inflammation. PloS one. 2013; 8:e61961. [PubMed: 23637937]
59. Herbert DR, Holscher C, Mohrs M, Arendse B, Schwegmann A, Radwanska M, Leeto M, Kirsch R, Hall P, Mossmann H, Claussen B, Forster I, Brombacher F. Alternative macrophage activation is essential for survival during schistosomiasis and downmodulates T helper 1 responses and immunopathology. Immunity. 2004; 20:623–635. [PubMed: 15142530]
60. Herbert DR, Orekov T, Roloson A, Ilies M, Perkins C, O'Brien W, Cederbaum S, Christianson DW, Zimmermann N, Rothenberg ME, Finkelman FD. Arginase I suppresses IL-12/IL-23p40-driven intestinal inflammation during acute schistosomiasis. Journal of immunology. 2010; 184:6438–6446.
61. Voelkel NF, Vandivier RW, Tuder RM. Vascular endothelial growth factor in the lung. American journal of physiology. Lung cellular and molecular physiology. 2006; 290:L209–L221. [PubMed: 16403941]
62. Semenza GL. Oxygen sensing, homeostasis, and disease. The New England journal of medicine. 2011; 365:537–547. [PubMed: 21830968]
63. Jung JE, Lee HG, Cho IH, Chung DH, Yoon SH, Yang YM, Lee JW, Choi S, Park JW, Ye SK, Chung MH. STAT3 is a potential modulator of HIF-1-mediated VEGF expression in human renal carcinoma cells. FASEB journal : official publication of the Federation of American Societies for Experimental Biology. 2005; 19:1296–1298. [PubMed: 15919761]
64. Xu Q, Briggs J, Park S, Niu G, Kortylewski M, Zhang S, Gritsko T, Turkson J, Kay H, Semenza GL, Cheng JQ, Jove R, Yu H. Targeting Stat3 blocks both HIF-1 and VEGF expression induced by multiple oncogenic growth signaling pathways. Oncogene. 2005; 24:5552–5560. [PubMed: 16007214]
65. Paulin R, Meloche J, Bonnet S. STAT3 signaling in pulmonary arterial hypertension. Jak-Stat. 2012; 1:223–233. [PubMed: 24058777]
66. Ramana CV, Kumar A, Enelow R. Stat1-independent induction of SOCS-3 by interferon-gamma is mediated by sustained activation of Stat3 in mouse embryonic fibroblasts. Biochem Biophys Res Commun. 2005; 327:727–733. [PubMed: 15649407]
67. Akira S. Roles of STAT3 defined by tissue-specific gene targeting. Oncogene. 2000; 19:2607–2611. [PubMed: 10851059]
68. Pauleau AL, Rutschman R, Lang R, Pernis A, Watowich SS, Murray PJ. Enhancer-mediated control of macrophage-specific arginase I expression. Journal of immunology. 2004; 172:7565–7573.
69. Rahman SM, Janssen RC, Choudhury M, Baquero KC, Aikens RM, de la Houssaye BA, Friedman JE. CCAAT/enhancer-binding protein beta (C/EBPbeta) expression regulates dietary-induced inflammation in macrophages and adipose tissue in mice. J Biol Chem. 2012; 287:34349–34360. [PubMed: 22902781]
70. Ruffell D, Mourkioti F, Gambardella A, Kirstetter P, Lopez RG, Rosenthal N, Nerlov C. A CREB-C/EBPbeta cascade induces M2 macrophage-specific gene expression and promotes muscle injury repair. Proc Natl Acad Sci U S A. 2009; 106:17475–17480. [PubMed: 19805133]
71. Huang GN, Thatcher JE, McAnally J, Kong Y, Qi X, Tan W, DiMaio JM, Amatruda JF, Gerard RD, Hill JA, Bassel-Duby R, Olson EN. C/EBP transcription factors mediate epicardial activation during heart development and injury. Science. 2012; 338:1599–1603. [PubMed: 23160954]

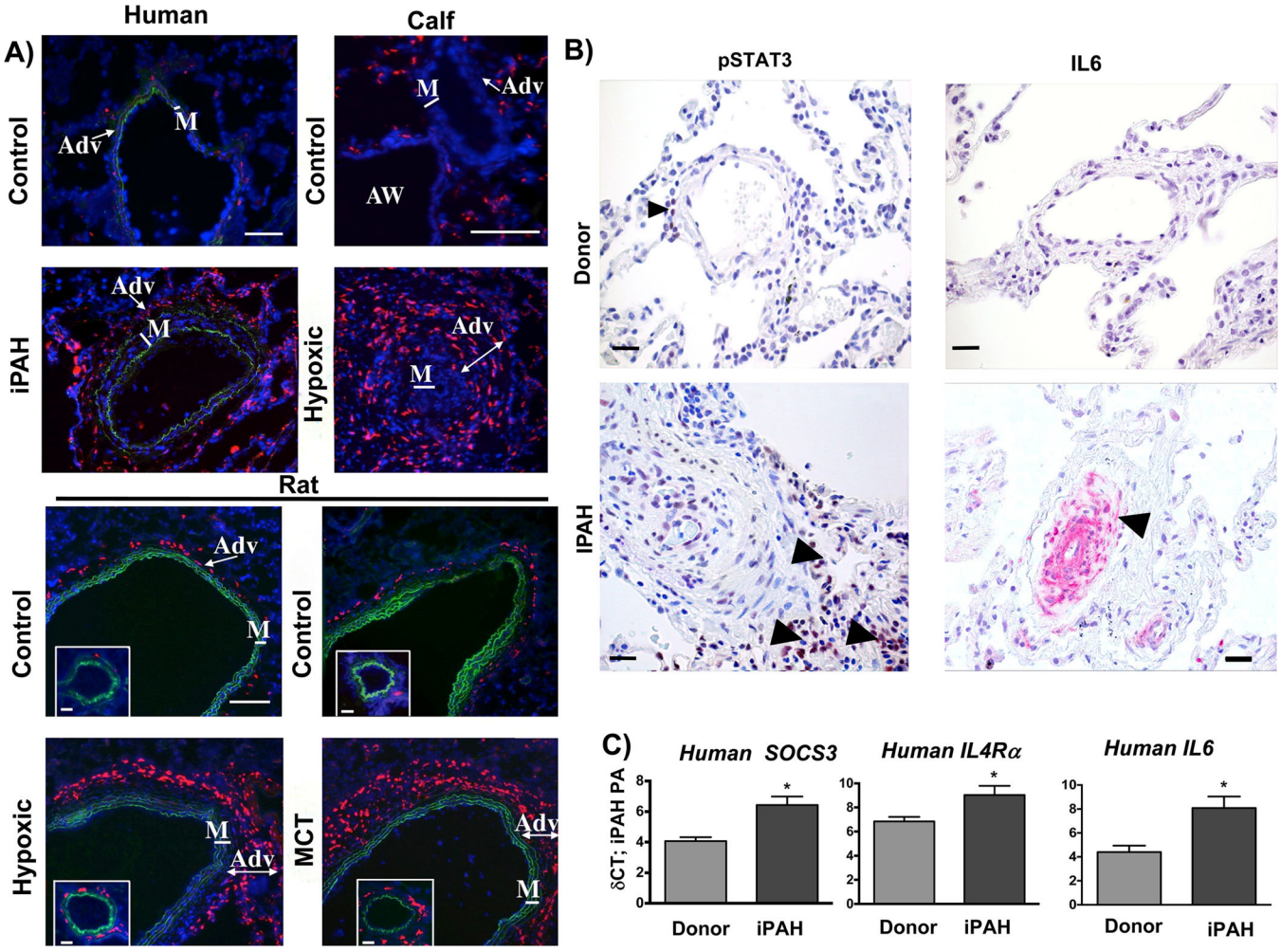

Figure 1. Adventitial macrophages in various forms of PH express CD163

(A) Accumulation of CD163-positive (human, calf) and ED2-positive (CD163 analog in rats) cells (red fluorescence) in human, calf and rat PAs. Note localization to the PA adventitia (Adv). All panels show DAPI counterstain (cell nuclei, blue) and autofluorescence of vascular elastic lamellae (green) defining borders of vascular media. Cryosections of hilar (human) or intra-lobar (calf, rat) PAs were immunostained. Controls (human donors or normoxic animals); iPAH (idiopathic pulmonary arterial hypertension), Hypoxic (experimental chronic hypoxia-induced PH), MCT (monocrotaline-induced PH). AW = airway; M = PA media. Scale bars = 100 μm

(B) Immunostaining for phosphorylated STAT3 and IL6 in formalin-fixed tissue from patients with iPAH and donor(s) as controls. Note adventitial staining for phosphorylated STAT3 and IL6 in PA from patients with iPAH (arrowheads). Images are representative of 8 patients and 5 donors. **(C)** Gene expression of canonical macrophage STAT3-regulated genes, *IL4Rα* and *SOCS3*, and the STAT3 inducer *IL6*, in laser-capture micro-dissected PA tissue from humans with iPAH and controls (Donor, both n= 8) expressed as δCt values normalized to expression of porphobilinogen deaminase (PBGD). **P* < 0.05 by unpaired two-tailed Student's *t*-test.

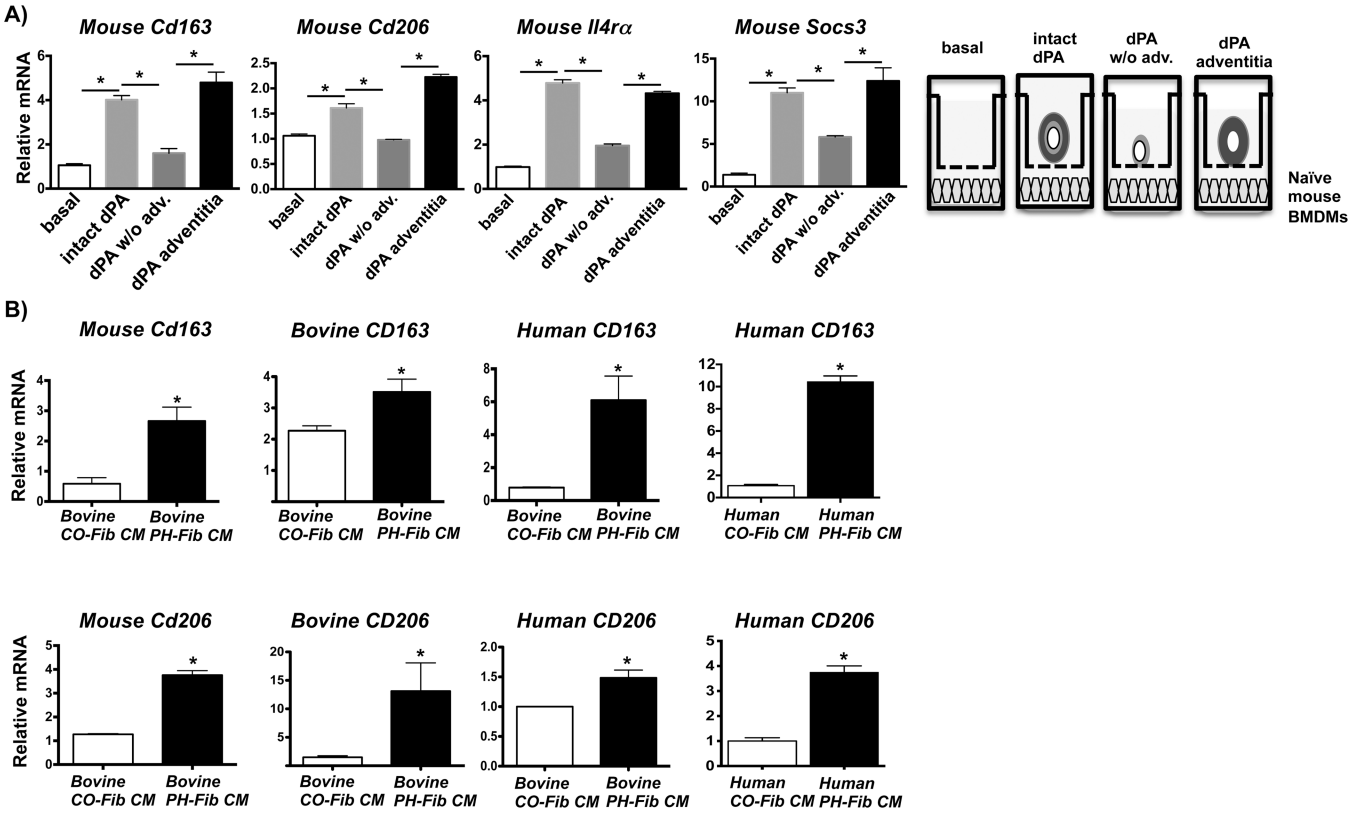

Figure 2. Adventitial fibroblasts activate macrophages

(A) Transwell experiment depicting mRNA expression in mouse bone marrow-derived macrophages (mouse BMDMs) exposed to soluble factors generated by distal pulmonary artery (dPA) explants from calves with chronic hypoxia-induced PH. dPAs were isolated such that an intact piece of PA tissue (intact dPA), a PA tissue piece from which the adventitia had been removed (dPA w/o adv.), and the removed adventitia piece itself (dPA adventitia) were incubated in the upper chamber of a 0.4-μm Transwell in the presence of naïve mouse BMDMs (lower chamber) for 16 h prior to RNA isolation and qRT-PCR (as depicted in the diagram). Displayed is the fold-induction (normalized to basal expression) of a representative PCR triplicate (average +/− SEM) from one of two calves. Three dPA segments were tested from each animal.. *$P < 0.05$ by one-way ANOVA. **(B)** Gene expression in BMDMs or monocytes exposed to conditioned media (CM) from dPA adventitial fibroblasts (PH-Fibs). Left panels top and bottom: CM from *ex vivo*-cultured bovine PH-Fibs (cells isolated from the dPA of calves with PH), and not from controls (CO-Fib CM) promotes gene expression of *Cd163* (top) and *Cd206* (bottom) in naïve mouse and bovine BMDMs; Right panels top and bottom: CM from bovine and human PH-Fibs induce expression of *Cd163* and *Cd206* in naïve human THP1 monocytes after 16 hrs of exposure. Relative mRNA levels are presented as mean±SEM of PCR triplicates after normalization to *Hprt1* expression and relative to gene expression in untreated macrophages/monocytes (basal) and are representative of at least n=5 experiments with CM from at least 3 different PH-Fibs and CO-Fibs populations isolated from at least 3 different animals/patients and using BMDMs from at least 3 different animals. *$P < 0.05$ by unpaired two-tailed Student's *t*-test.

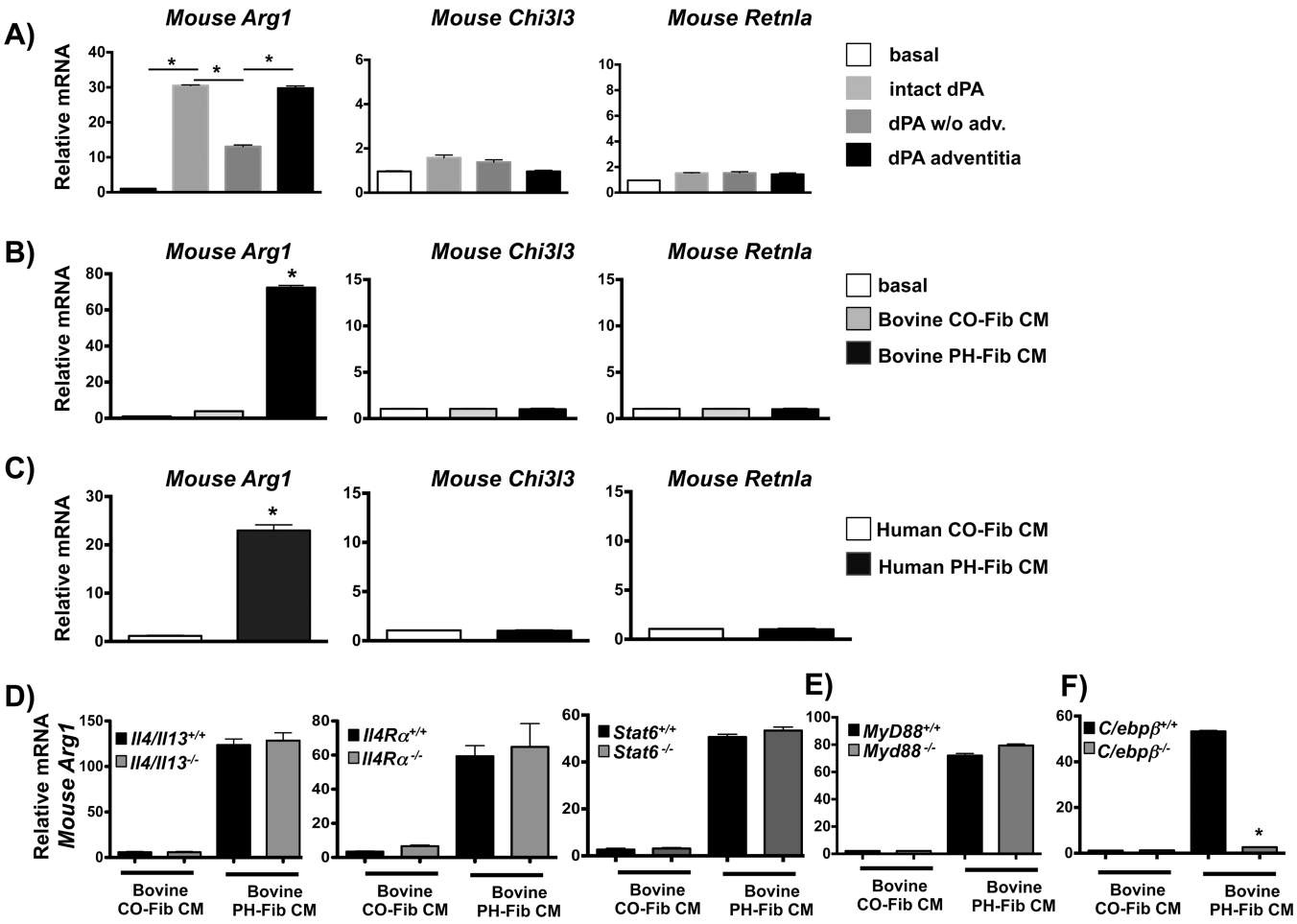

Figure 3. Fibroblast activated adventitial macrophages do not exhibit a canonical alternatively activated phenotype

(A) Soluble factors from the dPA adventitia (using dPA explants and 0.4-μm Transwells as in Fig. 2) induce gene expression of *Arg1*, but not *Chi3l3* and *Rentla* in mouse BMDMs. Displayed is the fold-induction (normalized to basal expression) of a representative PCR triplicate (average +/− SEM) from one of two calves. Three dPA segments were tested from each animal. **P* < 0.05 by one-way ANOVA. **(B, C)** PH-Fib CM, but not CO-Fib CM induces *Arg1*, but not *Chi3l3* or *Rentla* gene expression in mouse BMDMs (16 hr time point shown). The effect is similar with media generated from bovine (B) or human (C) PH-FIBs and CO-Fibs. Data are mean ± SEM of PCR triplicates after normalization to expression of *Hprt1* and relative to gene expression in untreated macrophages (basal). **P* < 0.05 by unpaired two-tailed Student's *t*-test. Presented is the result from a representative PH-Fib CM and a representative CO-Fib CM. They are representative of the results observed with 3 different cell populations (from different calves/patients) of each cell phenotype that were tested at least 3 times on BMDMs generated from at least 3 different mice. **(D, E).** Bovine PH-Fib CM induces comparable transcript levels for *Arg1* in WT BMDMs and BMDMs derived from *Il4/Il13*$^{-/-}$, *Il4ra*$^{-/-}$, or *Stat6*$^{-/-}$, and *Myd88*$^{-/-}$ mice. **(F)** *Arg1* expression in WT BMDMs is significantly attenuated in response to PH-Fib CM in BMDMs from *C/ebpβ*$^{-/-}$ mice. In D–F, PCR data are mean ± SEM from PCR triplicates after normalization

to expression of *Hprt1* (16hr time point) and expressed relative to gene expression in untreated macrophages (basal). Displayed are findings representative of experiments with CM from 3 PH-Fib and 3 CO-Fib populations repeated on BMDMs from 3 different animals. $*P < 0.05$ by one-way ANOVA.

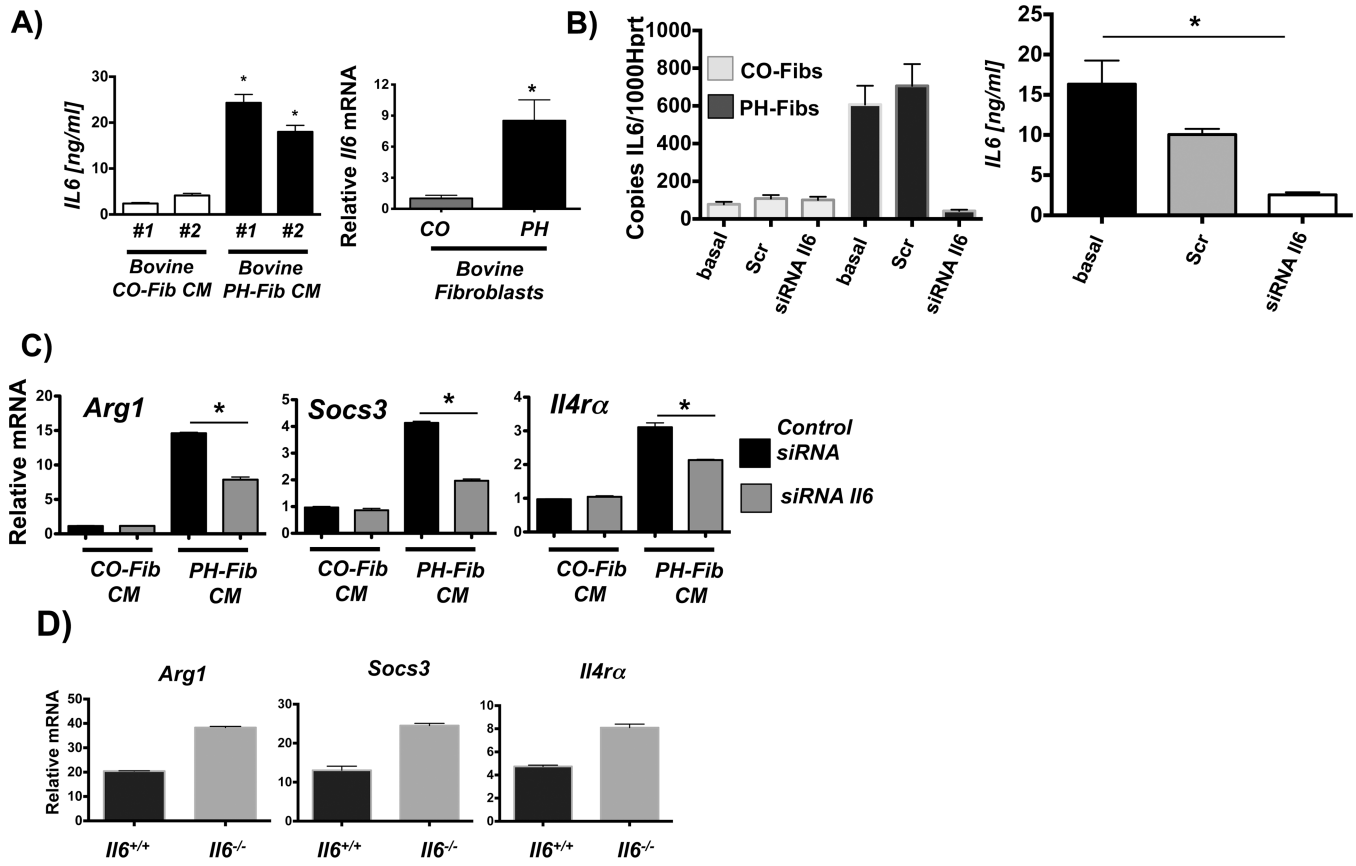

Figure 4. PH-Fibs activate macrophages through paracrine IL6

(A) IL6 protein amounts in CM from 2 bovine PH Fib populations; mean +/− SEM are shown from analysis of triplicate samples of each and compared to IL6 amounts in CM from 2 CO-Fibs, also tested in triplicate; * depicts $p< 0.05$ by t-test (PH-Fib CM vs. Cntrl CM); and relative *IL6* mRNA in bovine CO-Fib (normalized to 1, n=5) vs. PH-Fib (n=4); * depicts $p< 0.05$ by t-test. **(B)** siRNA mediated knock down of *IL6* transcription in bovine CO-Fibs and PH-Fibs; Scr=scrambled, basal=untreated; and IL6 protein amounts in CM from untreated (basal), scrambled, and IL6 siRNA treated PH-Fibs (n=3 each) tested in triplicate ELISA assay. **(C)** siRNA-mediated suppression of *IL6* gene transcription in bovine PH-Fibs limits the ability of CM to induce transcription of STAT3 regulated genes in WT mouse BMDMs. Gene expression is normalized to expression of *Hprt1* and relative to that in macrophages exposed to CM from CO-Fibs treated with control siRNA. Data are mean ± SEM from triplicate determinations and representative of two separate experiments. **(D)** Expression of STAT3 regulated genes, including *Hif1α*, in *WT* and *Il6*−/− BMDMs exposed for 16 hrs to bovine PH-Fib CM. *$P < 0.05$ by unpaired two-tailed Student's *t*-test of triplicate PCR analysis; one representative experiment with CM from one of three PH-Fib populations was tested on BMDMs from 3 different animals of each genotype.

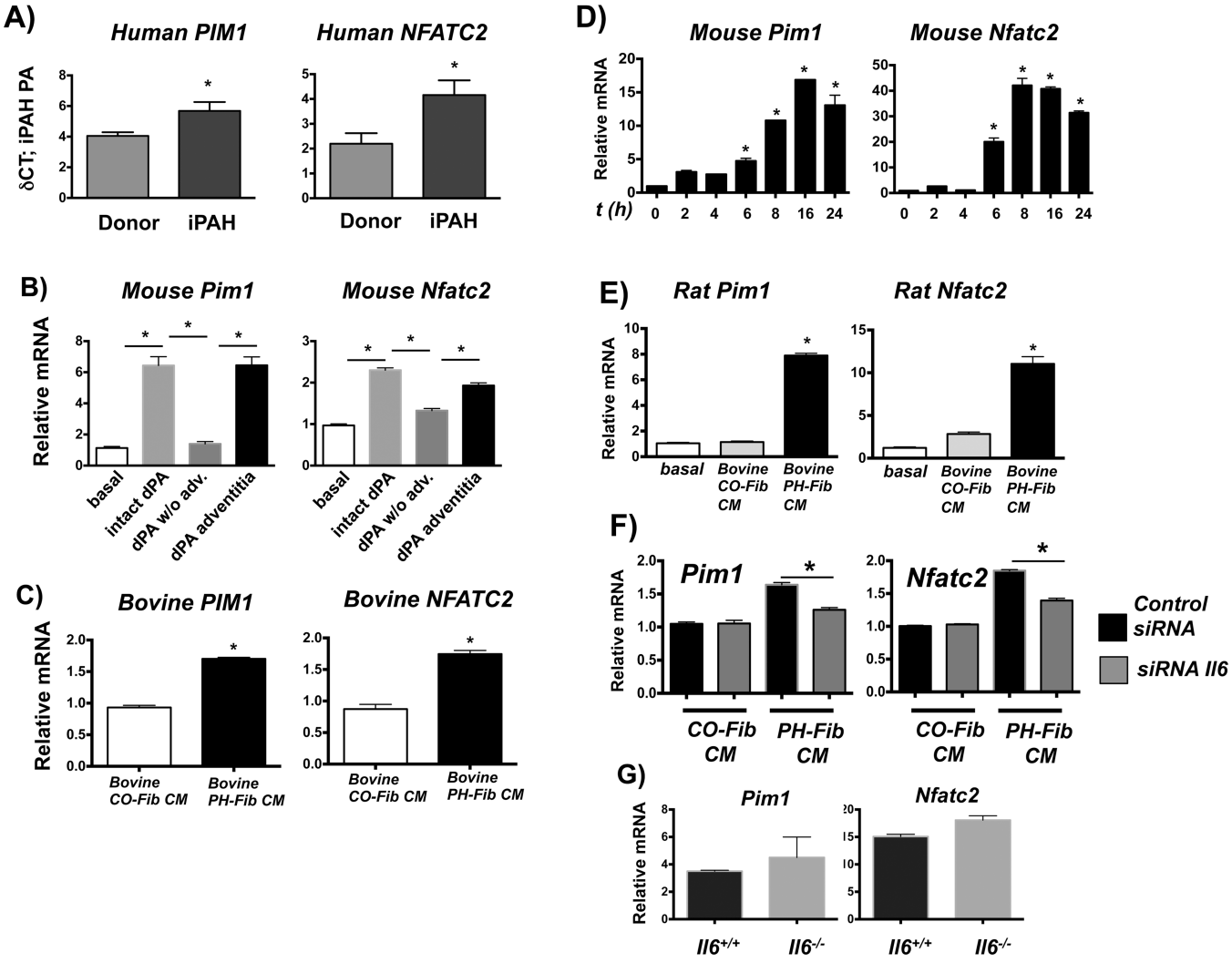

Figure 5. PIM1 and NFATC2 signaling is promoted in fibroblast-activated macrophages

(A) *PIM1* and *NFATC2* expression in laser-capture micro-dissected PA tissue from humans with iPAH compared to controls (both n= 8) expressed as δCt values normalized to expression of porphobilinogen deaminase (PBGD). **P* < 0.05 by unpaired two-tailed Student's *t*-test. **(B)** Soluble factors from the dPA adventitia (using dPA explants and 0.4-μm Transwells as in Fig. 2) induce gene expression of *Pim1* and *Nfatc2* in mouse BMDMs. Displayed is the fold-induction (normalized to basal expression) of a representative PCR triplicate (average +/− SEM) from one of two calves. Three dPA segments were tested from each animal; gene expression oafter incubation for 16hrs is shown. **P* < 0.05 by one-way ANOVA. **(C)** Bovine PH-Fib CM induces gene expression of *PIM1* and *NFATC2* in bovine (16hr time point shown), mouse (D, time course is shown), and rat (E; 16hr time point is shown) BMDMs. **(C–E)** Displayed are PCR triplicates of a representative experiment with one CO-Fib and one PH-Fib CM (mean ± SEM) normalized to *Hprt1* expression and expressed relative to basal (untreated) gene expression. These are representative of 3 experiments with CM from 3 separate CO-Fibs and 3 separate PH-Fibs cell populations on BMDMs from 3 different animals. **P* < 0.05 by unpaired two-tailed Student's *t*-test. **(F)**

siRNA-mediated suppression of *IL6* gene transcription in bovine PH-Fibs limits the ability of CM to induce transcription of *Pim1* and *Nfatc2* in WT mouse BMDMs. Gene expression is normalized to expression of *Hprt1* and relative to that in macrophages exposed to CM from CO-Fibs treated with control siRNA. Data are mean ± SEM from triplicate determinations and representative of two separate experiments. **(G)** Expression of *Pim1* and *Nfatc2* in *WT* and *Il6*−/− BMDMs exposed for 16 hrs to bovine PH-Fib CM. **P* < 0.05 by unpaired two-tailed Student's *t*-test of triplicate PCR analysis; one representative experiment with CM from one of three PH-Fib populations was tested on BMDMs from 3 different animals of each genotype.

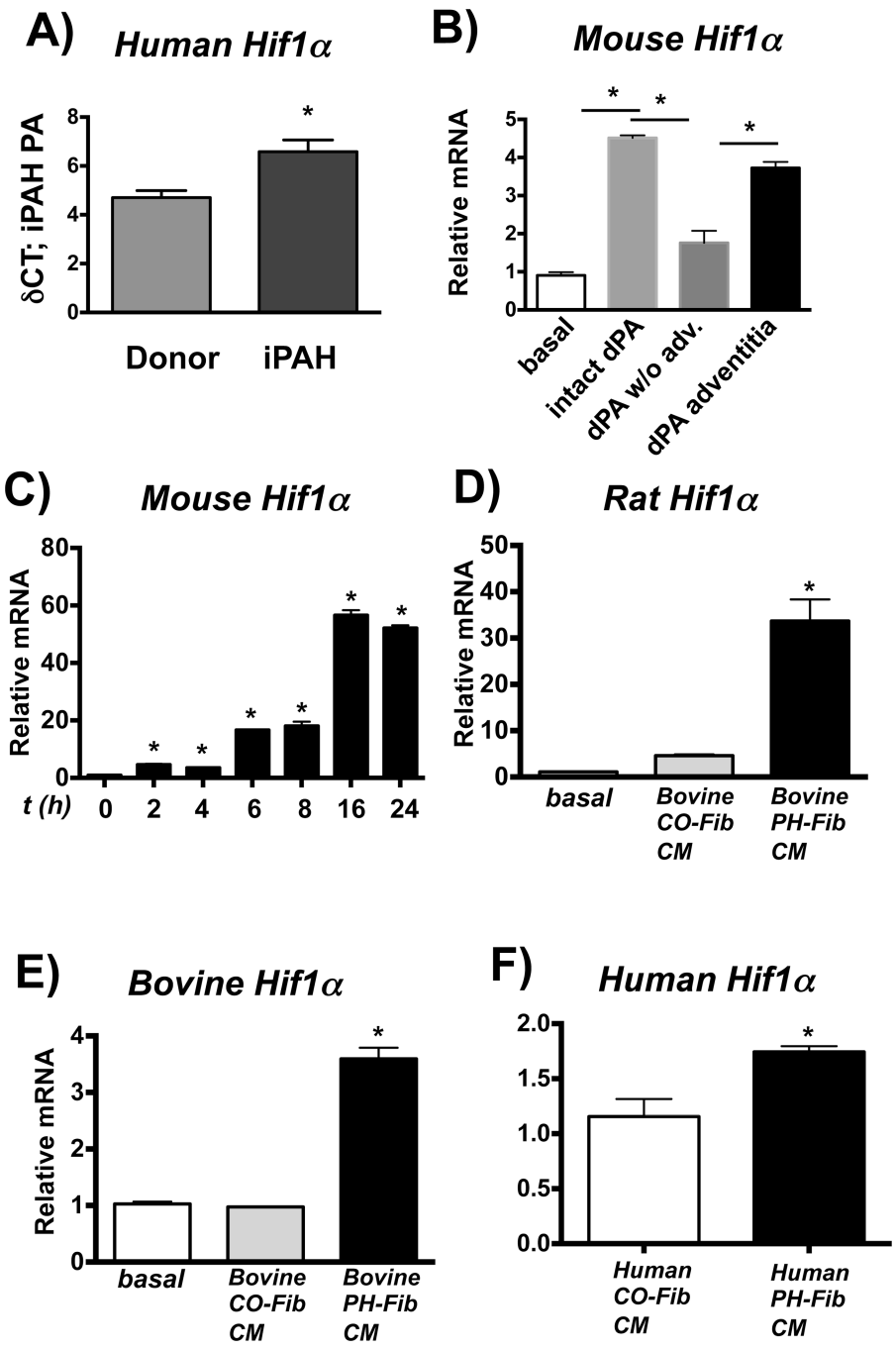

Figure 6. Hif1a is expressed in fibroblast-activated macrophages

(A) *HIF1a* gene expression in laser-capture micro-dissected PA tissue from humans with iPAH compared to controls (Donor, both n= 8) expressed as δCt values normalized to expression of porphobilinogen deaminase (PBGD). **P* < 0.05 by unpaired two-tailed Student's *t*-test. **(B)** Soluble factors from the dPA adventitia (using dPA explants from PH calves and 0.4-μm Transwells, as in Fig 2) induce gene expression of *Hif1a* in mouse BMDMs. Displayed is the fold-induction (normalized to basal expression) of a representative PCR triplicate (average +/− SEM) from one of two calves. Three dPA

segments were tested from each animal; 16hr time point is shown. **(C–E)** Bovine PH-Fib CM induces gene expression of *Hif1a* in mouse **(C; time course is shown)**, rat **(D; 16 hr time point)**, and bovine **(E; 16hr time point)** BMDMs. Displayed are PCR triplicates of a representative experiment with one CO-Fib and one PH-Fib CM (mean ± SEM) normalized to *Hprt1* expression and expressed relative to basal (untreated) gene expression. These are representative of 3 experiments with CM from 3 separate CO-Fibs and 3 separate PH-Fibs cell populations on BMDMs from 3 different animals. **(F)** *HIF1a* gene expression in human THP1 monocytes exposed to human PH-Fib CM compared to those exposed to human CO-Fib CM. Mean ± SEM of PCR triplicates CM from CO-Fibs and PH-Fibs after normalization to expression of *Hprt1* and expressed relative to CO-Fib CM induced gene expression; (16 hr exposure) **P* < 0.05 by unpaired two-tailed Student's *t*-test (A, F). * *P* < 0.05 by one-way ANOVA (B–E).

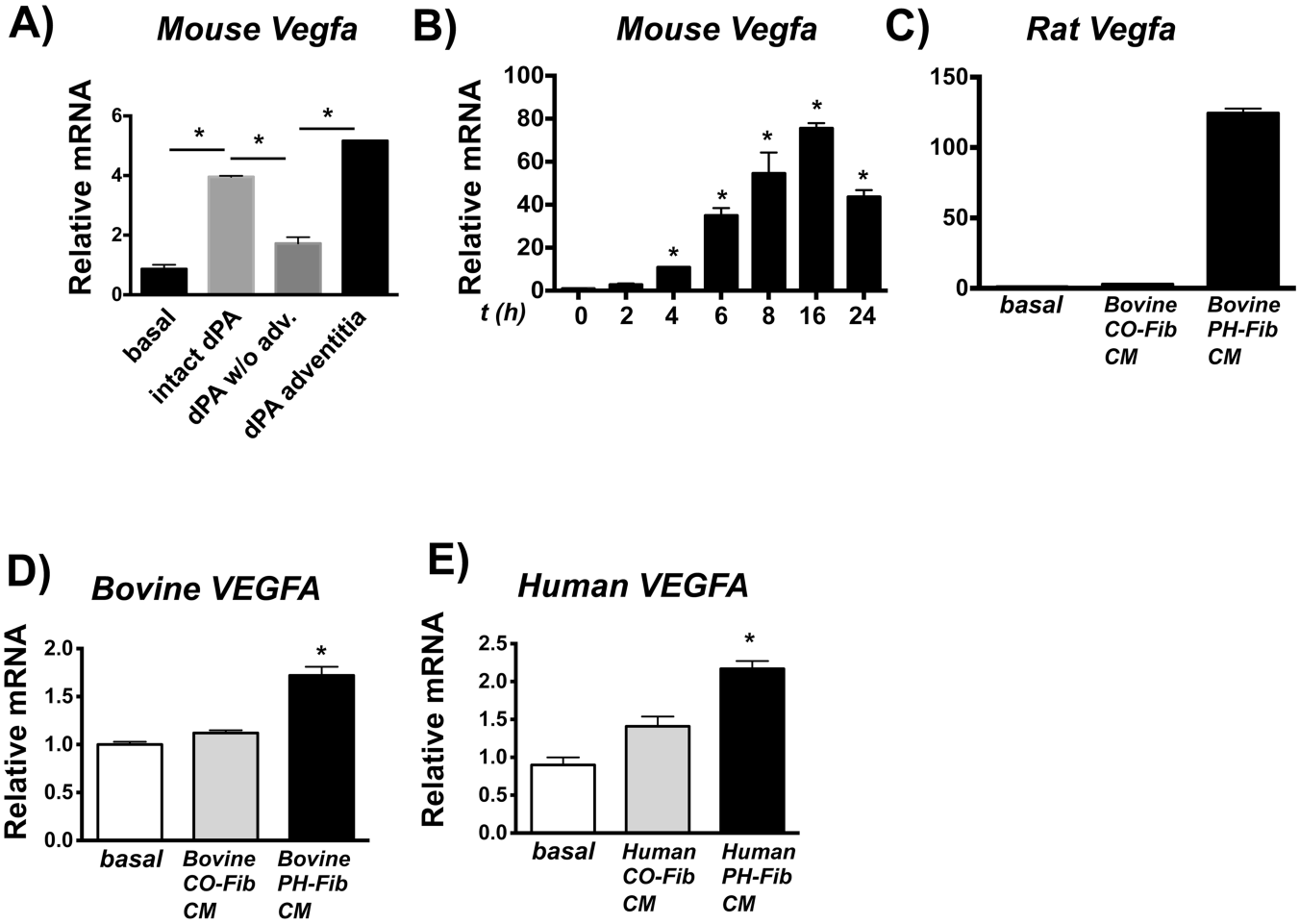

Figure 7. Vegfa is expressed in fibroblast-activated macrophages

(A) Soluble factors from the dPA adventitia (using dPA explants and 0.4-μm Transwells as in Fig. 2) induce gene expression of *Vegfa* in mouse BMDMs. Displayed is the fold-induction (normalized to basal expression) of a representative PCR triplicate (average +/− SEM) from one of two calves. Three dPA segments were tested from each animal; (16hr time point). **(B–D)** Bovine PH-Fib CM induces gene expression of *Hif1a* in mouse **(B; time course is shown)**, Rat **(C; 16 hr time point)**, and bovine **(D; 16hr time point)** BMDMs. Displayed are PCR triplicates of a representative experiment with one CO-Fib and one PH-Fib CM (mean ± SEM) normalized to *Hprt1* expression and expressed relative to basal (untreated) gene expression. These are representative of 3 experiments with CM from 3 separate CO-Fibs and 3 separate PH-Fibs cell populations on BMDMs from 3 different animals. **(E)** *VEGFa* gene expression in human THP1 monocytes exposed to human PH-Fib CM compared to those exposed to human CO-Fib CM. In E one representative experiment with CM from CO-Fibs and PH-Fibs isolated of at least 3 different patients/controls is shown. Data were obtained 16hrs after stimulation. **P* < 0.05 by ANOVA

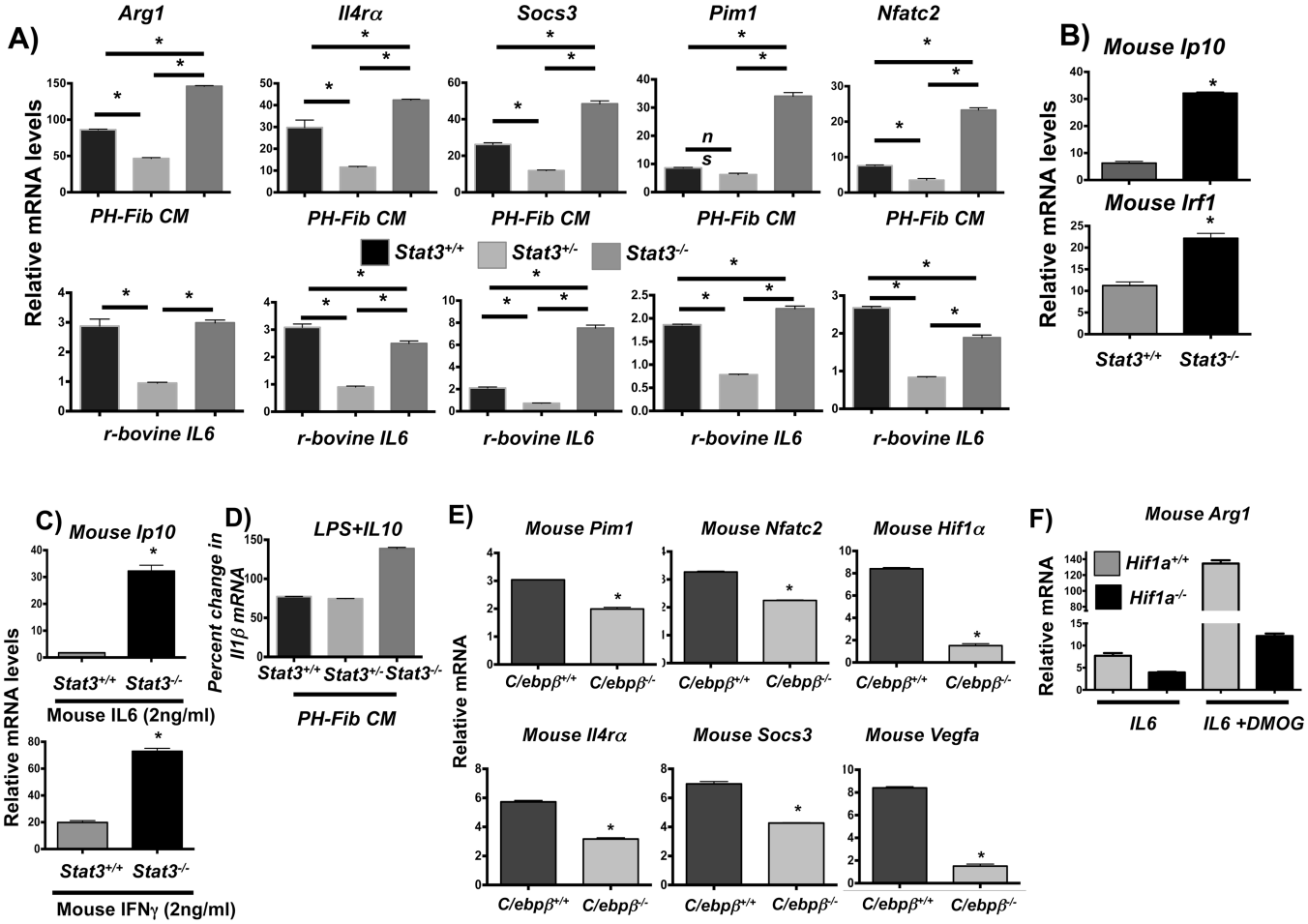

Figure 8. STAT3, C/EBPb, and HIF1a are critical regulators of fibroblast-mediated macrophage activation

(A) Transcription of *Arg1*, *Il4ra*, *Socs3*, *Pim1*, and *Nfatc2* in BMDMs from *Stat3*$^{fl/fl}$*Tie2cre* (designated *Stat3*$^{-/-}$) mice compared to BMDMs from WT mice *(Stat3*$^{+/+}$*)* and from *Stat3*$^{fl/+}$*Tie2cre* (designated *Stat3*$^{+/-}$) in response to bovine PH-Fib CM and recombinant bovine IL6 (2ng/ml) after stimulation for 16 hrs. (B) STAT1 target gene expression (*Ip10* and *Irf1*) in *Stat3*$^{-/-}$ compared to WT BMDMs in response to bovine PH-Fib CM after stimulation for 16 hrs. **(C)** STAT1 target gene expression (*Ip10*) in response to stimulation with mouse recombinant IL6 **(top panel)**, or mouse recombinant IFNγ **(bottom panel)** in *Stat3*$^{-/-}$ compared to WT BMDMs. **(D)** Percent gene expression of *Il1b* in WT, Stat3$^{+/-}$, and Stat3$^{-/-}$ BMDMs in response to LPS (100ng/ml)+IL10 (10ng/ml) compared to LPS (100ng/ml) alone (set as 100%) after 16 hrs of incubation. **(E)** Gene expression of *Pim1*, *Nfatc2*, *Hif1a*, *Il4ra*, *Socs3*, and *Vegfa* in *C/ebpb*$^{-/-}$ mouse BMDMs compared to WT BMDM in response to bovine PH-Fib CM after 16hrs of stimulation. **(F)** Expression of *Arg1* in *LysMcre* (designated *Hif1a*$^{+/+}$) and *Hif1a*$^{fl/fl}$*LysMcre* (designated *Hif1a*$^{-/-}$) mouse BMDMs in response to mouse recombinant IL6 (after stimulation for 16hrs) in the presence or absence of HIF stabilization with DMOG. Data are obtained from PCR triplicates and representative of results obtained from at least two different PH-Fib isolates and BMDMs

from 2 different animals. *$P < 0.05$ by unpaired two-tailed Student's *t*-test. *$P < 0.05$ by unpaired two-tailed Student's *t*-test.